Hydrogen sulfide mitigates ox-LDL-induced NLRP3/caspase-1/GSDMD dependent macrophage pyroptosis by S-sulfhydrating caspase-1

ZHENLI JIA[1*], XULIN ZHANG[2*], ZHIYI LI[1], HANYU YAN[1], XIANGQIN TIAN[3,4], CHENGHUA LUO[1], KETAO MA[1,3], LING LI[5] and LIANG ZHANG[1,3]

[1]Ministry of Education Key Laboratory of Xinjiang Endemic and Ethnic Diseases, Shihezi University, Shihezi, Xinjiang 832003, P.R. China; [2]Department of Blood Transfusion, Shenzhen Children's Hospital, Shenzhen, Guangdong 518034, P.R. China; [3]NHC Key Laboratory of Prevention and Treatment of Central Asia High Incidence Diseases, First Affiliated Hospital, School of Medicine, Shihezi University, Shihezi, Xinjiang 832008, P.R. China; [4]Henan Key Laboratory of Medical Tissue Regeneration, Xinxiang Medical University, Xinxiang, Henan 453003, P.R. China; [5]Department of Medical Morphology, Medical Teaching Experimental Center, School of Medicine, Shihezi University, Shihezi, Xinjiang 832000, P.R. China

Received August 2, 2023; Accepted April 19, 2024

DOI: 10.3892/mmr.2024.13259

Abstract. Macrophage pyroptosis mediates vascular inflammation and atherosclerosis (AS). Hydrogen sulfide (H_2S) exerts a protective role in preventing inflammation and AS. However, its molecular mechanisms of regulating the pyroptosis signaling pathway and inhibiting macrophage pyroptosis remain unexplored. The present study aimed to determine whether H_2S mitigates macrophage pyroptosis by downregulating the pyroptosis signaling pathway and S-sulfhydrating caspase-1 under the stimulation of oxidized low-density lipoprotein (ox-LDL), a pro-atherosclerotic factor. Macrophages derived from THP-1 monocytes were pre-treated using exogenous H_2S donors sodium hydrosulfide (NaHS) and D,L-propargylglycine (PAG), a pharmacological inhibitor of endogenous H_2S-producing enzymes, alone or in combination. Subsequently, cells were stimulated with ox-LDL or the desulfhydration reagent dithiothreitol (DTT) in the presence or absence of NaHS and/or PAG. Following treatment, the levels of H_2S in THP-1 derived macrophages were measured by a methylene blue colorimetric assay. The pyroptotic phenotype of THP-1 cells was observed and evaluated by light microscopy, Hoechst 33342/propidium iodide fluorescent staining and lactate dehydrogenase (LDH) release assay. Caspase-1 activity in THP-1 cells was assayed by caspase-1 activity assay kit. Immunofluorescence staining was used to assess the accumulation of active caspase-1. Western blotting and ELISA were performed to determine the expression of pyroptosis-specific markers (NLRP3, pro-caspase-1, caspase-1, GSDMD and GSDMD-N) in cells and the secretion of pyroptosis-related cytokines [interleukin (IL)-1β and IL-18] in the cell-free media, respectively. The S-sulfhydration of pro-caspase-1 in cells was assessed using a biotin switch assay. ox-LDL significantly induced macrophage pyroptosis by activating the pyroptosis signaling pathway. Inhibition of endogenous H_2S synthesis by PAG augmented the pro-pyroptotic effects of ox-LDL. Conversely, exogenous H_2S (NaHS) ameliorated ox-LDL-and ox-LDL + PAG-induced macrophage pyroptosis by suppressing the activation of the pyroptosis signaling pathway. Mechanistically, ox-LDL and the DTT increased caspase-1 activity and downstream events (IL-1β and IL-18 secretion) of the caspase-1-dependent pyroptosis pathway by reducing S-sulfhydration of pro-caspase-1. Conversely, NaHS increased S-sulfhydration of pro-caspase-1, reducing caspase-1 activity and caspase-1-dependent macrophage pyroptosis. The present study demonstrated the molecular mechanism by which H_2S ameliorates macrophage pyroptosis by suppressing the pyroptosis signaling pathway and S-sulfhydration of pro-caspase-1, thereby suppressing the generation of active caspase-1 and activity of caspase-1.

Correspondence to: Professor Liang Zhang, Ministry of Education Key Laboratory of Xinjiang Endemic and Ethnic Diseases, Shihezi University, 59 North 2nd Road, Shihezi, Xinjiang 832003, P.R. China
E-mail: zhangliang_0622@163.com

Ms. Ling Li, Department of Medical Morphology, Medical Teaching Experimental Center, School of Medicine, Shihezi University, 59 North 2nd Road, Shihezi, Xinjiang 832000, P.R. China
E-mail: lvhutao@126.com

*Contributed equally

Key words: hydrogen sulfide, pyroptosis, S-sulfhydration, macrophages, caspase-1

Introduction

Pyroptosis is a type of cell death that is considered to be highly pro-inflammatory and different from apoptosis (1-4). In contrast to apoptosis that without an inflammatory response, pyroptosis has a unique cellular morphology (i.e., nuclear integrity of pyroptotic cells is maintained)

and mechanism (1,2,4). Pyroptosis was initially identified in macrophages (5-7) and is characterized by membrane pore formation, cell membrane bubbling and swelling and substantial release of pro-inflammatory mediators or intracellular contents (2,8-11). Nucleotide-binding oligomerization domain-like receptor family pyrin domain containing 3 (NLRP3) inflammasome activation is involved in triggering canonical macrophage pyroptosis (2,4,9). When macrophages recognize pathogen-associated molecular patterns derived from pathogenic infection and molecular patterns related to damages induced by endogenous stress-associated signals, NLRP3 self-oligomerizes and binds to apoptosis-associated speck-like protein, which contains a caspase recruitment domain. This interaction recruits precursor of caspase-1 (pro-caspase-1) and leads to its cleavage and activation (12). Active caspase-1 is a key enzyme during pyroptosis that cleaves gasdermin D (GSDMD) and precursors of interleukin (IL)-1β and IL-18 to generate their biologically active forms (13,14). GSDMD serves as the central executor of pyroptosis, and its cleavage produces an N-terminal p31 fragment of GSDMD (GSDMD-N), which self-oligomerizes and creates membrane pores in cells (15). When these membrane pores form, intracellular substances including IL-1β and IL-18 are released, along with an influx of water, causing cell swelling and osmotic lysis (1,4,13,14). Simultaneously, pro-inflammatory mediators (IL-1β and IL-18) released by pyroptotic macrophages recruit inflammatory cells and further amplify the inflammatory response (9,16).

A mounting body of evidence reports that excessive macrophage pyroptosis exacerbates tissue damage and pathological inflammation (2,14,17), thereby contributing to initiation and progression of numerous types of inflammatory disorder, such as sepsis and kidney, neurodegenerative, liver and cardiovascular diseases (CVDs) (18,19). Several studies have reported the involvement of NLRP3/caspase-1/GSDMD-dependent macrophage pyroptosis in the development of atherosclerosis (AS) (1,4,6,8,10,13). Substantial evidence demonstrates that pyroptosis pathway-associated proteins, such as NLRP3, GSDMD and caspase-1 are prominently expressed in lesion macrophages both in animal and human AS (1,9,20-22). Moreover, risk factors associated with AS, including oxidized low-density lipoprotein (ox-LDL), homocysteine, cholesterol crystal and calcium phosphate can trigger NLRP3/caspase-1/GSDMD-dependent pyroptosis in macrophages (13,14,22-24). Pyroptosis of macrophages in early atherosclerotic lesions is reported to be beneficial as the death of macrophage attenuates the inflammatory response, scavenge cytotoxic lipoproteins and other harmful substances and decrease the synthesis of matrix metalloproteinases (4,25). However, sustained pyroptosis of macrophages in advanced atherosclerotic plaques facilitates formation of necrotic lipid cores and increases the instability of atherosclerotic lesions, resulting in plaque rupture and arterial thrombosis (25). The aforementioned findings demonstrate that macrophage pyroptosis is the predominant type of cell death in advanced atherosclerotic plaques (6). Furthermore, a growing body of evidence indicates that specific pharmacological inhibition or genetic intervention targeting the NLRP3/caspase-1/GSDMD axis can alleviate AS-associated risk factor-induced pyroptosis in macrophages and plaque development in apolipoprotein E $(ApoE)^{-/-}$ or low-density lipoprotein receptor $(Ldlr)^{-/-}$ mice (22,26-32). Therefore, elucidating the molecular mechanisms of pyroptosis in macrophages may enhance current understanding of the pathogenesis of CVDs, including AS (2) and pave the way for developing promising therapeutic strategies for a broad spectrum of inflammatory diseases, ranging from microbial infection to AS (13,33).

Hydrogen sulfide (H_2S), a gasotransmitter with multiple biological actions, exerts a key regulatory function in multiple physiological and pathophysiological events, including cell death, differentiation, proliferation, hypertrophy, metabolism, stress responses, inflammation, angiogenesis and vasodilation (34-36). Evidence suggests that both endogenous H_2S and several exogenous H_2S donors exert notable vasodilatory, pro-angiogenic, anti-hypertensive and anti-atherosclerotic effects by diverse mechanisms including anti-oxidation, anti-inflammation and pro- and anti-apoptosis (34,36-39). Malfunction of endogenous H_2S production is associated with numerous CVDs (36,38). Exogenous H_2S and H_2S derived from macrophages exert anti-inflammatory and anti-pyroptotic effects in *in vivo* and *in vitro* conditions as a response to pro-inflammatory or pro-atherogenic stimuli. Previous studies have reported that this is achieved by suppressing NLRP3 inflammasome activation (40-43), however the underlying mechanisms by which H_2S directly regulates macrophage pyroptosis remains unclear. S-sulfhydration of functional proteins induced by H_2S is suggested as a key mechanism responsible for the biological effects of H_2S (34,44). H_2S mediated S-sulfhydration of multiple critical target proteins (Liver kinase B1, specificity protein 1, NF-κB, Parkin and Kelch-like ECH-associated protein 1 and c-Jun) in numerous cellular signaling pathways (AMP-activated protein kinase pathway, apoptotic pathway, Ldlr protein pathway and NLRP3 inflammasome pathway) is involved in cell differentiation, cell proliferation/hypertrophy, cell metabolism, cell survival/death, inflammation and oxidative stress (34,44). However, whether H_2S inhibits macrophage pyroptosis and exerts anti-inflammatory effects through the S-sulfhydration of pyroptosis pathway-associated proteins remains uncertain.

The present study used ox-LDL-stimulated THP-1 macrophages to establish an *in vitro* model that mimics AS-induced macrophage pyroptosis according our previous study (45). The impact of exogenous H_2S donors and inhibition of endogenous H_2S production on NLRP3/caspase-1/GSDMD-mediated macrophage pyroptosis in response to ox-LDL stimulation was assessed. Pyroptosis-related morphological features, propidium iodide (PI)-positive staining, lactate dehydrogenase (LDH) release, caspase-1 activity and expression and secretion of pyroptosis pathway-specific proteins and pro-inflammatory cytokines were evaluated. Furthermore, the mechanisms via which H_2S serves its anti-pyroptotic role in THP-1 macrophages through S-sulfhydrating caspase-1 were assessed.

Materials and methods

Cell culture. Human THP-1 monocytic cells were purchased from National Collection of Authenticated Cell Cultures (cat. no. SCSP-567; The Chinese Academy of Sciences; https: //cellbank.org.cn/search-detail.php?id=517). THP-1 cells were cultured in RPMI-1640 medium (cat. no. C11875500BT;

Gibco; Thermo Fisher Scientific, Inc.) supplemented with 10% fetal bovine serum (FBS; cat. no. 10270-106; Gibco; Thermo Fisher Scientific, Inc.) and 1% penicillin/streptomycin (cat. no. SV30010; HyClone; Cytiva). The culture was incubated at 37˚C with 5% CO_2.

Differentiation of THP-1 monocytes into macrophages. For differentiation, THP-1 monocytes were plated in 6-($1x10^6$ cells/well), 12-($1x10^5$ cells/well) or 96-well culture plates ($1x10^4$ cells/well) containing RPMI-1640 medium, 10% FBS and 1% penicillin/streptomycin for subsequent cultivation. THP-1 monocytes were incubated with phorbol-12-myristate-13-acetate (PMA; cat. no. P6741; Beijing Solarbio Science & Technology Co., Ltd.) for 24 h at 37˚C. Adherent differentiated THP-1 cells were rinsed with PBS and incubated at 37˚C for a further 24 h in RPMI-1640 complete media without PMA.

Cell viability assay. THP-1 macrophages were seeded ($1x10^5$ cells/ml) in 96-well plates (100 μl/well) in a 37˚C incubator. After 24 h, the cells were treated with increasing concentrations of NaHS (50, 100, 200 and 400 μM; cat. no. 161527; MilliporeSigma), D,L-propargylglycine (PAG) (1.0, 2.5, 5.0 and 10.0 μM; cat. no. P7888; MilliporeSigma) and ox-LDL (25, 50, 100 and 150 μg/ml; cat. no. YB-002, http://www.yiyuanbiotech.com/PRO.asp?id=562#section2; Guangzhou Yiyuan Biological Technology Co., Ltd.) for 24 h in a 37˚C incubator. Cell viability was assessed using Cell Counting Kit-8 (cat. no. K1018; APeXBIO Technology LLC) according to the manufacturer's instructions. A total of 10 μl CCK-8 reagent was added to each well and incubated for 2 h at 37˚C. Optical density (OD) was measured at 450 nm with a xMark microplate spectrophotometer (Bio-Rad Laboratories, Inc.). For each treatment group, cells were seeded in triplicate. Cell viability was calculated according to the manufacturer's instructions.

Drug treatment. THP-1 macrophages were classified into six groups as follows: Control, cells were cultured with RPMI-1640 for 24 h at 37˚C; ox-LDL, cells were incubated with 100 μg/ml ox-LDL at 37˚C for 24 h to construct an *in vitro* model of pyroptosis or activate the caspase-1-dependent pyroptosis signaling pathway; PAG, cells were treated with 2.5 mM PAG supplemented in RPMI-1640 medium for 24 h at 37˚C; ox-LDL + NaHS, cells were pretreated with 200 μM NaHS for 30 min before treatment with 100 μg/ml ox-LDL for 23.5 h at 37˚C; ox-LDL + PAG, the cells were pretreated with 2.5 mM PAG for 30 min at 37˚C prior to ox-LDL treatment for 23.5 h; and ox-LDL + PAG + NaHS, where cells were pretreated with 200 μM NaHS and 2.5 mM PAG for 30 min before treatment with ox-LDL for 23.5 h at 37˚C.

In supplementary experiments containing NaHS and/or lipopolysaccharide (LPS) + adenosine triphosphate (ATP) treatment, THP-1 macrophages were classified into the following four groups: Control, THP-1 cells were cultured with RPMI-1640 for 24 h at 37˚C; NaHS, cells were treated with 200 μM NaHS for 24 h at 37˚C; lipopolysaccharide (LPS; cat. no. L2880; MilliporeSigma) + ATP (cat. no. 6419; MilliporeSigma), cells were first treated with 1 μg/ml LPS for 18 h and subsequently treated with 5 mM ATP at 37˚C for 6 h to construct an *in vitro* model of pyroptosis; and LPS + ATP + NaHS, cells were pretreated with 200 μM NaHS for 30 min, then treated with 1 μg/ml LPS for 18 h at 37˚C, before pyroptosis was triggered by treatment with 5 mM ATP for 5.5 h.

To determine whether H_2S inhibits caspase-1 activity by sulfhydrating pro-caspase-1, THP-1 cells were allocated into the following groups: Control, THP-1 cells were treated with PBS for either 2 or 24 h at 37˚C; NaHS, THP-1 cells were exposed to 200 μM NaHS for 2 h at 37˚C; dithiothreitol (DTT)/ox-LDL, THP-1 cells were treated with 1 mM DTT (cat. no. 43816; MilliporeSigma) for 2 h or incubated with 100 μg/ml ox-LDL for 24 h at 37˚C; ox-LDL + NaHS, THP-1 cells were pretreated with 200 μM NaHS for 30 min, followed 100 μg/ml ox-LDL for an additional 23.5 h at 37˚C; and DTT + NaHS, THP-1 cells were treated with 1 mM DTT for 1.5 h at 37˚C after the pretreatment with 200 μM NaHS for 30 min.

Measurement of H_2S concentration. H_2S concentration in THP-1 cells was assessed by a H_2S detection kit (cat. no. A146-1-1; Nanjing Jiancheng Bioengineering Institute), which uses the classical methylene blue method, according to the manufacturer's instructions. THP-1 cells ($1x10^6$ cells/well) were seeded in a 60-mm culture dish and cultured overnight at 37˚C. Cells were incubated with the aforementioned treatments for 24 h and lysed using 1 ml PBS (pH 7.4) via ultrasonication (ultrasonic treatment five times, 8 sec at intervals of 10 sec, 1.5 min in total) on ice. Subsequently, a 100 μl aliquot of the cell lysate was transferred into a centrifuge tube with 1% w/v zinc acetate and 12% NaOH to incubate for 90 min in a shaking metal bath at 37˚C. Bradford protein assay kit (cat. no. P0006C; Beyotime Institute of Biotechnology) was used to ascertain the protein concentration in the cell lysates. After adding 20 mM N,N-dimethyl-p-phenylenediamine sulfate and 30 mM $FeCl_3$ containing 1.2 M HCl at room temperature for 15 min, the reaction was halted. Then, 10% trichloroacetic acid was added to precipitate protein and the mixture was centrifuged for 5 min at 10,000 x g and at room temperature. Using a xMark™ microplate spectrophotometer (Bio-Rad Laboratories, Inc.), absorbance of the resultant methylene blue in the supernatant was measured at 665 nm. The H_2S concentration in each sample was calculated as follows: H_2S (nmol/mg protein)=[(absorbance of the sample-absorbance of the blank)/0.0044] x [total reaction volume/(sample volume x protein concentration of the sample)].

Cell death assay. Micrographs of pyroptotic cell morphology were captured under phase microscopy using a 40X objective prior to cell harvesting. The proportion of pyroptosis-like cells was obtained by the number of cells displaying pyroptotic morphology relative to the total cell count in five randomly selected fields/well, each containing ~50 cells. These experiments were performed at least three times independently.

The morphological changes associated with pyroptosis and pyroptotic cell death were assessed by Hoechst 33342/PI staining using a fluorescent microscope (TH4-200; Olympus Corporation) and LDH activity assay using a spectrophotometer (xMark; Bio-Rad Laboratories, Inc.). Each experiment was independently conducted at least three times. Specifically, for Hoechst 33342/PI double staining, THP-1 cells ($5x10^5$ cells/well) were treated with the aforementioned drugs for 24 h. Cells were then washed with PBS and stained

using 10 μl Hoechst 33342 staining solution from Hoechst 33342/PI dual staining kit (cat. no. G023-1-1; Nanjing Jiancheng Bioengineering Institute) at 37˚C for 10 min without light. Next, cells were stained using 5 μl PI (cat. no. G023-1-1; Nanjing Jiancheng Bioengineering Institute) at 25˚C for 10 min without light. Cells were subsequently washed three times with PBS and images of were captured under a TH4-200 fluorescent microscope (Olympus Corporation) at a magnification of x200. Image J software (version 1.46r; National Institutes of Health) was used to count PI-stained cells in five randomly selected microscopic fields. Cells were quantified as follows: PI-stained cells (%)=(number of red fluorescent cells/total blue fluorescent cells) x100.

LDH activity in the culture medium was measured using an LDH activity assay kit (cat. no. A020-2-2; Nanjing Jiancheng Bioengineering Institute). Cell culture supernatants (200 μl/sample) were harvested and centrifuged at 400 x g for 5 min at 4˚C. Then, 20 μl supernatant was added to a 96-well test plate and mixed with 5 μl coenzyme I or deionized water and 25 μl substrate buffer. The mixture was then incubated at 37˚C for 15 min. Then 25 μl 2,4-dinitrophenylhydrazine was added and samples incubated at 37˚C for 15 min. Finally, 250 μl 0.4 M NaOH solution was added and the mixture was incubated at 25˚C for 5 min. The absorbance was measured at 450 nm with a xMark microplate spectrophotometer (Bio-Rad Laboratories, Inc.). The proportion of LDH release was calculated according to the manufacturer's instructions.

Measurement of caspase-1 activity. THP-1 cells were incubated with the aforementioned treatments for 2 or 24 h and caspase-1 activity was assessed using a caspase-1 activity assay kit (cat. no. C1102; Beyotime Institute of Biotechnology). The cells were lysed with the kit lysis buffer on ice for 15 min and centrifuged at 18,000 x g for 15 min at 4˚C. Protein content in each sample was determined using a Bradford protein assay kit (cat. no. P0006C; Beyotime Institute of Biotechnology). Then, 40 reaction buffer and 10 μl 2 mM caspase-1 substrate were added to 50 μl supernatant, incubated at 37˚C for 2 h and the amount of yellow formazan pNA was measured at 405 nm using a xMark microplate spectrophotometer (Bio-Rad Laboratories, Inc.). Caspase-1 activity was calculated according to the manufacturer's instructions, which was represented as fold-change in activity compared with the control.

Immunofluorescent staining. To determine if macrophages expressed active caspase-1, immunofluorescence staining was performed. THP-1 cells were treated with the aforementioned treatments for 24 h. THP-1 cells were fixed for 15 min at 25˚C with 4% paraformaldehyde and rinsed with PBS (three times at 5 min per time). The cells were permeabilized for 3 min at room temperature using 0.2% Triton X-100, and then blocked with 5% BSA (cat. no. SW3015; Beijing Solarbio Science & Technology Co., Ltd.) at 37˚C for 30 min in a humidified incubating box. Then, cells were incubated with antibodies against cleaved caspase-1 (1:200; cat. no. PA5-99390; Thermo Fisher Scientific, Inc.) overnight at 4˚C. Following PBS washes (three times at 5 min per time), cells were incubated for 1.5 h at 37˚C without exposure to light with a FITC-conjugated secondary antibody (1:100; cat. no. ZF-0311; OriGene Technologies, Inc.). Nuclei were counterstained with 1 μg/ml DAPI at room temperature for 15 min without light. Images were captured at a magnification of x200 under a TH4-200 fluorescence microscope (Olympus Corporation). The average fluorescence intensity (AFI) value was calculated to assess the expression of active caspase-1 in THP-1 cells using Image J software (version 1.46r; National Institutes of Health).

Immunoblotting. After incubating the THP-1 cells with the aforementioned treatments for 24 h, total secreted proteins were extracted from the culture medium using the methanol/chloroform method, as previously described (46,47). THP-1 cells were collected by centrifugation at 800 x g for 10 min at 4˚C and lysed in ice-cold RIPA lysis buffer (cat. no. R0010; Beijing Solarbio Science & Technology Co., Ltd.) supplemented with protease inhibitor cocktail (cat. no. P8340; MilliporeSigma) and incubated at 4˚C for 20 min. The supernatants from the cell lysates were isolated by centrifugation at 12,000 x g for 15 min at 4˚C and the protein concentration of the supernatants was examined using a BCA protein assay kit (cat. no. 23227; Thermo Fisher Scientific, Inc.). Protein pellets from cell-free media were dissolved in 2X Laemmli buffer and the cell lysates of THP-1 cells were mixed with 5X Laemmli buffer. Samples were denatured at 98˚C for 5 min. Equal amounts of protein (40 μg/lane) were loaded onto 10% (more than 60 kDa of molecular weight) or 12% (15-60 kDa of molecular weight) SDS-PAGE gels and separated by electrophoresis. The separated proteins were transferred to polyvinylidene fluoride (PVDF) membranes (cat. nos. ISEQ00010 (0.22 μm), and IPVH00010 (0.45 μm); MilliporeSigma) with the pore size of 0.22 and 0.45 μm using a wet-transfer system. The membranes were blocked at 25˚C for 2 h using 5% skimmed milk, then incubated overnight at 4˚C with primary antibodies against NLRP3 (1: 1,000; cat. no. ab263899; Abcam), pro-caspase-1 (1:1,000; cat. no. PA5-87536; Thermo Fisher Scientific, Inc.), cleaved caspase-1 (1:1,000; cat. no. PA5-99390; Thermo Fisher Scientific, Inc.), GSDMD (1:1,000; cat. no. ab210070; Abcam), cleaved GSDMD (1:1,000; cat. no. 36425S; Cell Signaling Technology, Inc.), pro-IL-1β (1:500; cat. no. ab315084; Abcam), IL-1β (1:1,000; cat. no. 83186; Cell Signaling Technology, Inc.), IL-18 (1:1,000; cat. no. A1115; ABclonal Biotech Co., Ltd.), β-actin (1:1,000; cat. no. TA-09; OriGene Technologies, Inc.) and GAPDH (1:1,000; cat. no. TA-08; OriGene Technologies, Inc.) in 5% BSA buffer (cat. no. SW3015; Beijing Solarbio Science & Technology Co., Ltd.). The membranes were then washed three times with TBST (tris-buffered saline with 0.05% Tween-20) solution and incubated for 2 h at 25˚C with secondary antibody (1:10,000; cat. nos. ZB-2301, and ZB-2305; OriGene Technologies, Inc.) conjugated with horseradish peroxidase. After rinsing the membranes five times with TBST (tris-buffered saline with 0.05% Tween-20), proteins bands were visualized with an enhanced chemiluminescence detection kit (cat. no. WBKLS0100; Merck KGaA) via X-ray film exposure or a Tanon 5200 chemiluminescence imaging system (Tanon Science and Technology Co., Ltd.) Image J software (version 1.46r; National Institutes of Health) was used to assess and quantify the relative integrated OD (IOD) of the protein bands as well as the relative expression levels of the target proteins. To detect secreted active caspase-1 and IL-1β, following the SDS-PAGE electrophoresis for total secreted proteins extracted from the cell free media, the upper part of the gel (>40 kDa) was stained by Coomassie brilliant blue to indicate loading of lanes, and the lower part (<40 kDa) was transferred to

a PVDF membrane for the detection of secreted caspase-1 and IL-1β by western blotting. Coomassie brilliant blue staining from total secreted protein blots was applied as a loading control for culture supernatant (48,49) and GAPDH or β-actin acted as the loading control for the cell lysates.

Quantification of NLRP3 and pyroptosis-specific cytokines. To assess NLRP3 inflammasome activation and secretion of pyroptosis-related pro-inflammatory cytokines, PMA-differentiated THP-1 macrophages were seeded into 12-well plates ($5x10^5$ cells/well) and incubated with 100 μg/ml ox-LDL for 23.5 h at 37˚C, in the presence or absence of 200 μM NaHS and/or 2.5 mM PAG pretreatment for 30 min. THP-1 cells were lysed in ice-cold RIPA lysis buffer (cat. no. R0010; Beijing Solarbio Science & Technology Co., Ltd.) and incubated at 4˚C for 15 min. The supernatant obtained from the cell lysates was isolated via centrifugation at 18,000 x g for 15 min at 4˚C. The protein concentration of the supernatants from THP-1 cell lysate was determined using a BCA protein assay kit (cat. no. 23227; Thermo Fisher Scientific, Inc.). Furthermore, cell-free culture supernatant (500 μl/sample) was immediately collected by centrifugation at 300 x g for 5 min at 4˚C and frozen at -80˚C. ELISA kits were used according to the manufacturer's instructions to quantify the concentrations of NLRP3 (cat. no. ab274401; Abcam) in THP-1 cell lysate and the levels of IL-1β (cat. no. EK101B; MultiSciences Biotech Co., Ltd.) and IL-18 (cat. no. EK118; MultiSciences Biotech Co., Ltd.) in cell culture medium. Precoated 96-well plates and ELISA reagents were brought to room temperature. Standards and 100 μl cell culture supernatants were added to each well of the microplate, and precoated with biotinylated monoclonal antibodies against IL-1β or IL-18 (1:100) for 10 min at 25˚C. The microplates were incubated with continuous shaking for 2 h at room temperature, then rinsed with washing buffer for six times. Subsequently, 100 μl HRP-conjugated streptavidin (1:100) was added to each well and incubated in the dark at room temperature for 45 min with gentle shaking. The wells were washed six times and 100 μl tetramethylbenzidine solution was added to each well and incubated for 30 min at room temperature with no exposure to light. Finally, 100 μl stop solution was added to each well and the maximum absorbance values at 450 nm or reference absorbance values at 570/630 nm were measured with a xMark microplate spectrophotometer (Bio-Rad Laboratories, Inc.). The expression levels of NLRP3, IL-1β and IL-18 in THP-1 cells or cell culture medium were determined using the standard curve established from the kit standards.

Biotin switch assay for determination S-sulfhydration of pro-caspase-1. The S-sulfhydration of pro-caspase-1 was assessed using the biotin switch test described by Mustafa *et al* (50), with minor adjustments. THP-1 cells were harvested by centrifugation at 800 x g for 10 min at 4˚C and washed twice with ice-cold PBS following treatment with or without ox-LDL, DTT or/and NaHS for 2 or 24 h as aforementioned, The cells were then kept on ice and homogenized using ultrasonication (sonicated three times, 15 sec each time, 1 min in total) in an ice-cold HEN [N-2-hydroxyethylpiperazine-N'-2-ethanesulfonic acid (HEPES)/ethylene diamine tetraacetic acid (EDTA)/Neocuproine] buffer containing protease inhibitor cocktail (cat. no. P1050; Beyotime Institute of Biotechnology), 250.0 HEPES-NaOH, 1.0 EDTA and 0.1 mM neocuproine and 100.0 μM deferoxamine. The cell lysate was cleared by centrifugation at 14,000 x g at 4˚C for 15 min and protein concentration in the supernatant was measured using the Pierce BCA Protein Assay kit (cat. no. 23227; Thermo Fisher Scientific, Inc.). Cell lysate containing 800 μg total protein was combined with 2 ml of HEN buffer [250.0 HEPES (pH 7.7), 1.0 EDTA and 0.1 mM neocuproine and 100.0 μM deferoxamine], supplemented with 2.5% SDS and 20 mM S-methyl methanethiosulfonate (MMTS) and incubated at 50˚C for 30 min with gentle and frequent vortexing to block the free thiol (-SH). The blocked proteins were incubated with 8 ml cooled acetone at -20˚C for 30 min. The free MMTS plus acetone were removed by centrifugation at 3,000 x g for 10 min at 4˚C. The precipitated proteins were washed three times with 8 ml ice-cold acetone and resuspended in 2 ml HEN buffer supplemented with 1% SDS. The sample was then mixed with 0.4 mM biotin-N-[6-(biotinamido) hexyl]-3'-(2'-pyridyldithio) propionamide (cat. no. 21341; Thermo Fisher Scientific, Inc.) in DMSO and incubated for 3 h at 25˚C. After that, cooled acetone was added into the biotin-labeled proteins to incubated for 40 min at -20˚C. The proteins were centrifuged at 3,000 x g for 10 min at 4˚C and rinsed with 2 ml ice-cold acetone and resuspended in 1 ml neutralization buffer (25 HEPES-NaOH, 1 EDTA and 100 mM NaCl and 0.5% Triton X-100).

The samples were incubated with 20 μl streptavidin-agarose beads (cat. no. S1638; MilliporeSigma) on a rotator mixer overnight at 4˚C to capture S-sulfhydrated proteins. Samples were then centrifuged at 800 x g for 5 min at 4˚C, and the supernatant was discarded. The precipitated pellet of streptavidin-agarose beads was then resuspended in 1 ml HEN buffer containing 1% SDS and centrifuged for 5 min at 800 x g at 4˚C. S-sulfhydrated proteins were then washed five times with 1 ml HEN buffer supplemented with 1% SDS, and spun down at 800 x g for 5 min at 4˚C. The S-sulfhydrated proteins of samples were eluted from the streptavidin-agarose beads by 2X SDS-PAGE loading buffer (3% SDS, 1% β-mercaptoethanol, 62.5 mM tris-base, and 0.005% bromophenol blue) at 37˚C for 20 min on the rotator mixer. The S-sulfhydrated proteins of samples were denatured at 98˚C for 5 min and separated on 12% SDS-PAGE gels, and transferred to a PVDF membrane (cat. no. ISEQ00010; MilliporeSigma) with a pore size of 0.22 μm. The membranes were blocked at 25˚C for 2 h using 5% skimmed milk, and S-sulfhydrated proteins underwent western blot analysis using a pro-caspase-1-specific antibody (1:1,000; cat. no. ab207802; Abcam). GAPDH (1:1,000; cat. no. TA-08; OriGene Technologies, Inc.) acted as the loading control. The procedure of western blot analysis for S-sulfhydrated pro-caspase-1 was the same as for immunoblotting of pro-caspase-1 expression. Samples were run on SDS-PAGE gels alongside the total target protein ('input') that had not been subjected to the biotin switch assay procedure. The same antibodies were used for western blotting to quantify S-sulfhydrated proteins. The ratio of S-sulfhydrated pro-caspase-1 IOD relative to total pro-caspase-1 IOD was densitometrically analyzed using Image J software (version 1.46r; National Institutes of Health) and calculated to represent the relative S-sulfhydration levels of pro-caspase-1.

Statistical analysis. GraphPad Prism 8 (version 8.0.2; Dotmatics) was used to analyze data. All data are presented

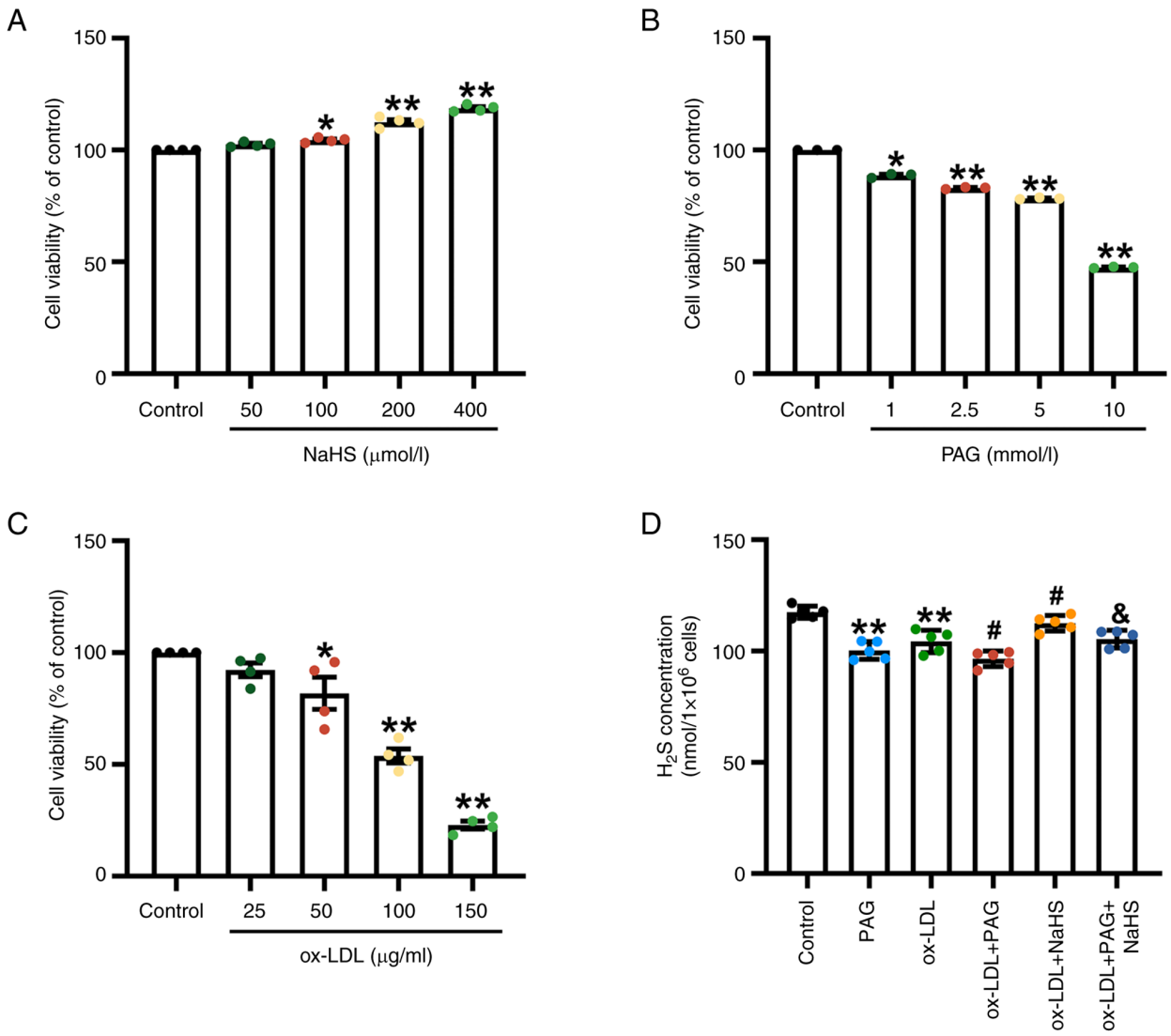

Figure 1. Effect of NaHS, PAG and ox-LDL on cytotoxicity and H_2S levels in PMA-differentiated THP-1 macrophages. (A) The different concentrations of NaHS (50, 100, 200 and 400 μM) treatment alone for 24 h increases viability of THP-1 macrophages (n=4). (B) Cell viability was determined in THP-1 cells treated with PAG at different concentrations of 1.0, 2.5, 5.0 and 10.0 μM for 24 h (n=3). (C) The effects of ox-LDL on the viability of THP-1 macrophages. THP-1 cells were incubated with the different concentrations of ox-LDL (25, 50, 100 and 150 μg/ml) for 24 h (n=4). Cell Counting Kit-8 was used to measure the cell viability of the macrophages. The viability of the control was normalised to 100%. (D) NaHS increases H_2S concentration in THP-1 macrophages treated by ox-LDL or ox-LDL + PAG. THP-1 macrophages were stimulated with 100 μg/ml ox-LDL for 23.5 h in the presence or absence of pretreatment with 200 μM NaHS and/or 2.5 mM PAG for 30 min. H_2S levels were assessed using a methylene blue method-based H_2S detection kit in THP-1 macrophages (n=5). *P<0.05 and **P<0.01 vs. control, $^{\#}$P<0.05 vs. ox-LDL, $^{\&}$P<0.05 vs. ox-LDL + PAG. PAG, D,L-propargylglycine; ox-LDL, oxidized low-density lipoprotein; PMA, phorbol-12-myristate-13-acetate.

as the mean ± SEM of >3 independent experiments performed under identical conditions. The statistical significance between two groups was assessed using the unpaired two-tailed Student's t test in cell viability assay and comparisons between multiple groups was analyzed by one-way ANOVA followed by Bonferroni's post hoc test. P<0.05 was considered to indicate a statistically significant difference.

Results

NaHS increases cell viability or H_2S concentration in THP-1 macrophages with or without ox-LDL stimulation, while PAG and ox-LDL reduces them. Cytotoxicity of NaHS, PAG and ox-LDL toward THP-1 macrophages was assessed by the CCK-8 assay. THP-1 macrophages were treated with NaHS, PAG and ox-LDL for 24 h. Compared with the control group, 100, 200 and 400 μM NaHS significantly increased the viability of THP-1 macrophages (Fig. 1A), whereas treatment with PAG (1, 2.5, 5 or 10 mM) (Fig. 1B) and ox-LDL (50, 100 and 150 μg/ml) (Fig. 1C) for 24 h resulted in a significant decrease in cell viability of THP-1 macrophages. Concentrations of 200 μM NaHS, 2.5 mM PAG and 100 μg/ml ox-LDL were used in subsequent assays.

The main enzyme synthesizing endogenous H_2S in macrophages is cystathionine-γ-lyase (CSE) (42,51,52). Dysfunction in the CSE/H_2S pathway induced by ox-LDL is associated with ox-LDL-induced inflammation in macrophage (51,53). Therefore, ox-LDL and the CSE inhibitor PAG were used in the present study. To assess whether exogenous H_2S donors and the inhibition of endogenous H_2S synthesis impact H_2S production

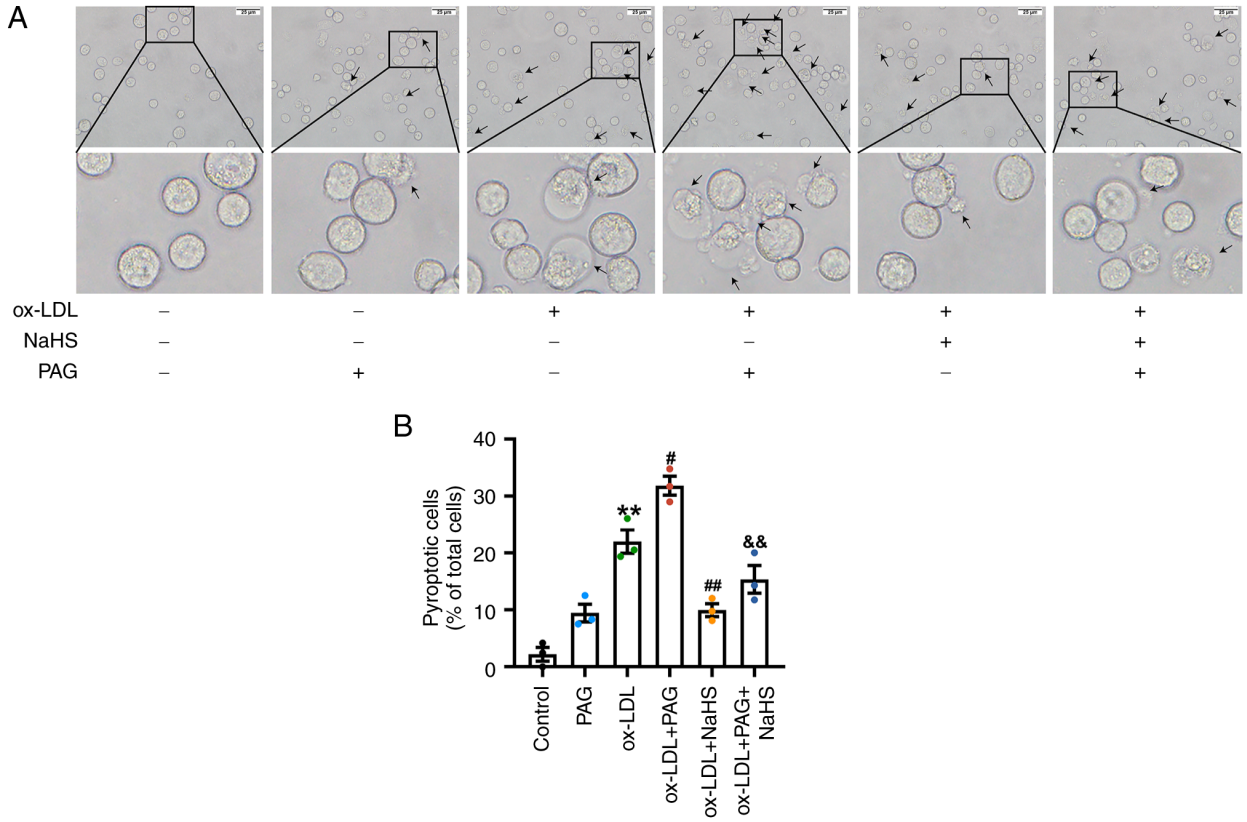

Figure 2. H_2S signaling suppresses pyroptosis-like morphological changes in ox-LDL-treated THP-1 macrophages. Differentiated THP-1 macrophages were stimulated with 100 μg/ml ox-LDL for 23.5 h in the presence or absence of pretreatment with 200 μM NaHS and/or 2.5 mM PAG for 30 min. (A) Effect of H_2S signaling on the morphological characteristics associated with pyroptosis in ox-LDL-treated THP-1 cells was assessed using an optical microscope. Representative bright-field/phase-contrast images of pyroptotic THP-1 cells are shown in the upper panel, and enlarged views are shown in the lower panel. The black arrowheads indicate typical pyroptotic cells. Magnification, x400; scale bar, 25 μm. (B) Percentage of pyroptosis was calculated by counting the number of pyroptotic cells (based on morphology) relative to the number of total cells in five random fields, each containing ~50 cells. n=3. **P<0.01 vs. control, $^{\#}$P<0.05, $^{\#\#}$P<0.01 vs. ox-LDL and $^{\&\&}$P<0.01 vs. ox-LDL + PAG. ox-LDL, oxidized low-density lipoprotein; PAG, D,L-propargylglycine.

in ox-LDL-stimulated THP-1 macrophages, H_2S concentration was measured using methylene blue assay. Compared with the control group, ox-LDL and PAG treatment alone significantly inhibited endogenous H_2S production in THP-1 cells (Fig. 1D). ox-LDL + PAG treatment significantly reduced H_2S production compared with the ox-LDL group. However, pretreatment with an exogenous H_2S donor significantly increased H_2S concentrations compared with the ox-LDL group (Fig. 1D). Similarly, NaHS pretreatment also led to an increased H_2S content in the presence of a combination of ox-LDL and PAG compared with the ox-LDL + PAG group (Fig. 1D).

H_2S signaling suppresses pyroptotic cell death in THP-1 macrophages exposed to ox-LDL and LPS + ATP. Although the impact of H_2S on pyroptosis in numerous types of cell has been partially elucidated in previous studies (41,54-56), its morphological and biological influence on pyroptosis in macrophages remains unclear. To assess the role of exogenous and endogenous H_2S in pyroptosis induced by ox-LDL and LPS + ATP in macrophages, THP-1 macrophages were pretreated with 200 μM NaHS and/or 2.5 mM PAG for 30 min, then treated with 100 μg/ml ox-LDL or 1 μg/ml LPS + 5 mM ATP for 23.5 h. Changes in cell morphology associated with pyroptosis were assessed using an optical microscope. THP-1 cells in the control group exhibited normal morphology (Figs. S1A and 2A). NaHS (200 μM) or PAG (2.5 mM) treatment alone under the same concentration showed no significant effect on morphology of macrophages compared with the control group (Figs. S1A and 2A). By contrast, ox-LDL and LPS + ATP induced a significant increase in the typical pyroptotic death of THP-1 cells compared with the control group (Figs. S1 and 2), characterized by pronounced cell swelling or membrane rupture and balloon-shaped bubbles extending from the plasma membrane (Figs. S1A and 2A). Meanwhile, THP-1 cells from ox-LDL + PAG group exhibited more obvious cell morphology associated with pyroptosis and a more percentage of pyroptotic THP-1 cells compared with the ox-LDL group (Fig. 2). However, pretreatment with NaHS significantly decreased ox-LDL and LPS + ATP induced morphological changes associated with pyroptosis and reduced the percentage of pyroptotic THP-1 cells (Figs. S1 and 2). In addition, the pretreatment of NaHS also effectively improved cell morphology associated with pyroptosis, and reduced the percentage of pyroptotic THP-1 cells in the presence of a combination of ox-LDL and PAG compared with those in the ox-LDL + PAG group (Fig. 2).

To further assess the impact of H_2S signaling on pyroptosis in macrophages induced by ox-LDL and LPS + ATP, Hoechst 33342/PI double staining in THP-1 cells and LDH activity in the culture supernatant was assessed. PI enters the cell via the ruptured membrane (57). ox-LDL significantly increased the

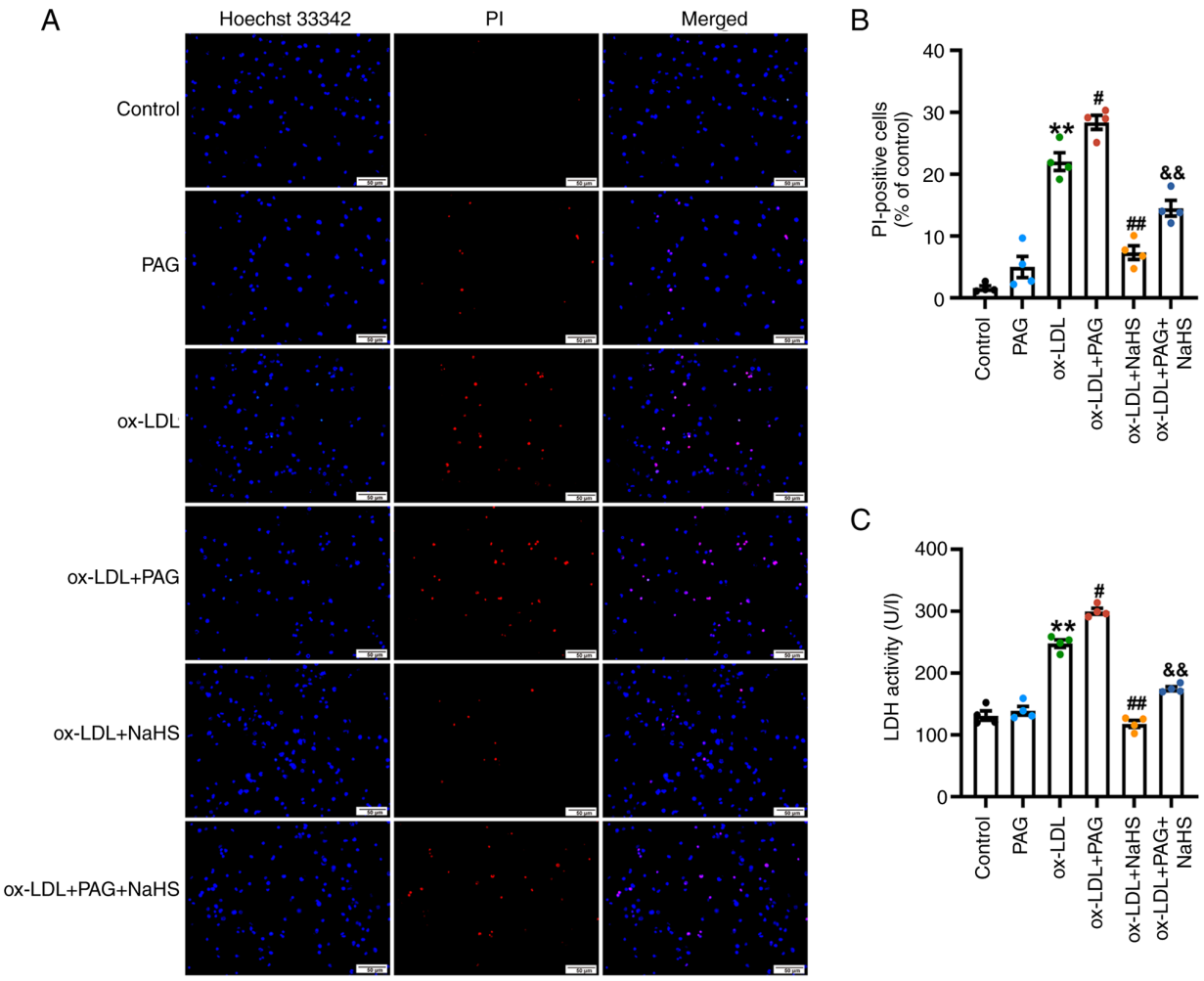

Figure 3. H_2S signaling inhibits ox-LDL-induced pyroptosis in THP-1 macrophages. PMA-differentiated THP-1 macrophages were stimulated with 100 μg/ml ox-LDL for 23.5 h in the presence or absence of pretreatment with 200 μM NaHS and/or 2.5 mM PAG for 30 min. (A) NaHS inhibits ox-LDL or ox-LDL + PAG -induced increase in the percentage of PI-positive cells. Pyroptotic death in THP-1 cells was evaluated by Hoechst 33342/PI double staining. Images were observed using fluorescence microscopy. Magnification, x200; scale bar, 50 μm. (B) Proportion of pyroptotic cells was determined by PI-positive dead cells relative to the total number of live cells exhibiting blue fluorescence, demonstrated by Hoechst 33342 staining. n=4. (C) NaHS inhibits LDH release in THP-1 macrophages treated by ox-LDL or ox-LDL + PAG. Pyroptosis was assessed by measuring LDH activity in the cell free media. n=4. **P<0.01 vs. control, $^{\#}$P<0.05, $^{\#\#}$P<0.01 vs. ox-LDL and $^{\&\&}$P<0.01 vs. ox-LDL + PAG. ox-LDL, oxidized low-density lipoprotein; PMA, phorbol-12-myristate-13-acetate; PAG, D,L-propargylglycine; PI, propidium iodide; LDH, lactate dehydrogenase.

percentage of PI-positive THP-1 cells (Fig. 3A and B) and LDH release (Fig. 3C) compared with the control. The percentage of PI-positive cells was significantly increased in the ox-LDL + PAG group compared with the ox-LDL group (Fig. 3A and B). Likewise, LDH release was also significantly increased in the ox-LDL + PAG compared with the ox-LDL group (Fig. 3C).

NaHS (200 μM; Fig. S2) or PAG treatment alone (2.5 mM; Fig. 3) under the same concentration did not affect the percentage of PI-positive cells or LDH release. These results suggested that ox-LDL induced pyroptosis in macrophages derived from THP-1, consistent with a prior study that reported that differentiated THP-1 macrophages exhibit increased pyroptosis in response to different ox-LDL concentrations (50, 100 and 150 μg/ml) (45).

NaHS lowered the proportion of PI-positive cells (Fig. 3A and B) and LDH release (Fig. 3C) in ox-LDL + NaHS group compared with those of the ox-LDL group in THP-1 cells. Additionally, compared with ox-LDL + PAG treatment group, NaHS pretreatment significantly inhibited the increase in the proportion of PI-positive cells (Fig. 3A and B) and LDH release (Fig. 3C) in THP-1 cells from ox-LDL + PAG + NaHS group. Similarly, the percentage of pyroptotic cells and LDH release in the LPS + ATP + NaHS group was significantly lower compared with the LPS + ATP group, suggesting LPS + ATP-induced macrophage pyroptosis could be attenuated by NaHS pretreatment (Figs. S1 and S2). In summary, these results suggested that H_2S signaling protected macrophages from pyroptotic cell death induced by ox-LDL.

H_2S signaling inhibits caspase-1 expression and activity in ox-LDL and LPS + ATP stimulated THP-1 macrophages. Caspase-1 is a key enzyme in the canonical pyroptotic pathway. Caspase-1 cleaves GSDMD, generating the active GSDMD-N form, which forms pores in the cell membrane, initiating pyroptosis (27). To validate whether H_2S directly modulates caspase-1, the role of H_2S signaling in intracellular localization of cleaved caspase-1 as well as caspase-1 activity in THP-1 macrophages was assessed.

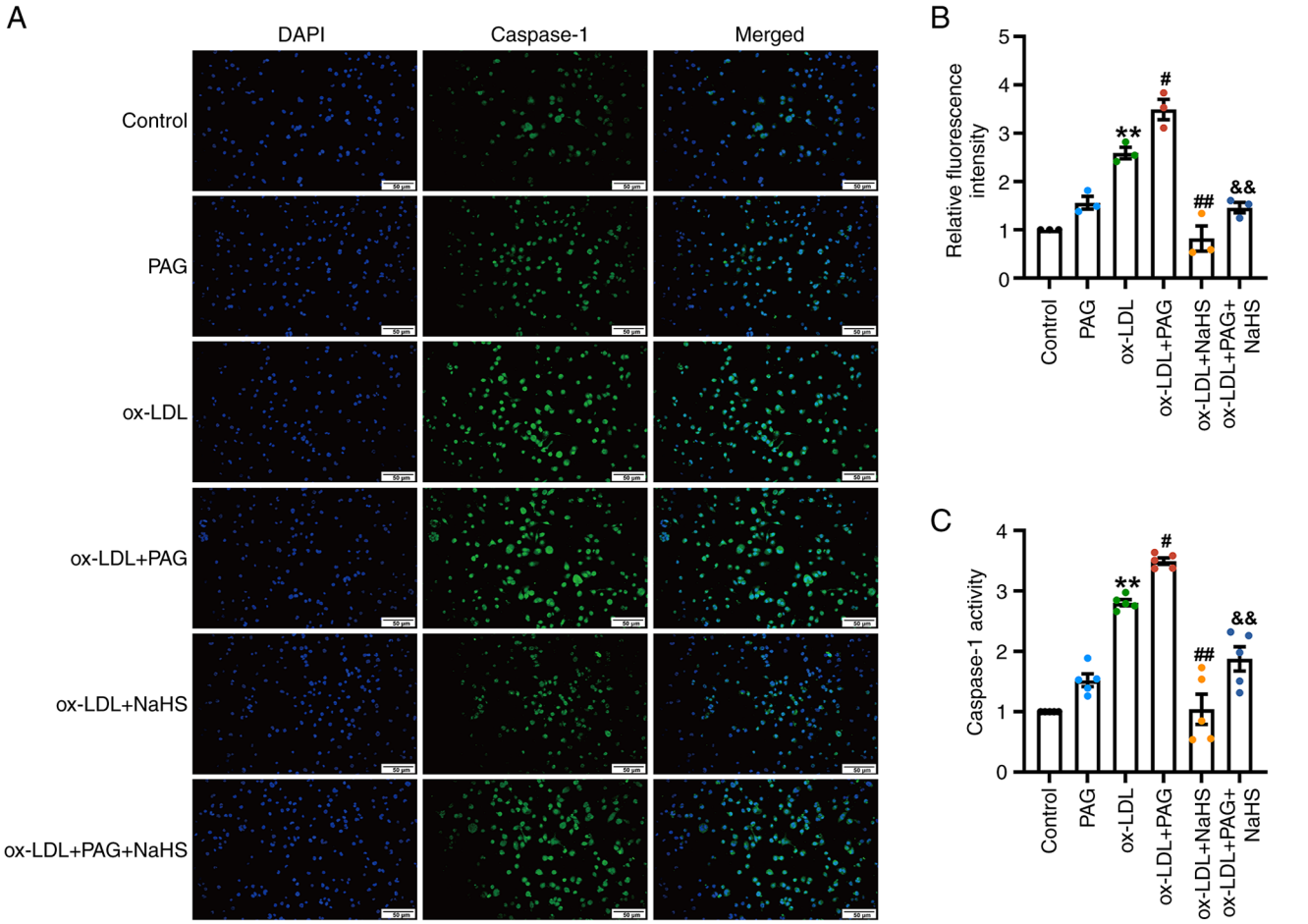

Figure 4. H_2S signaling inhibits activation and enzymatic activity of caspase-1 in THP-1 macrophages stimulated by ox-LDL. PMA-primed THP-1 cells were exposed to 100 μg/ml ox-LDL for 23.5 h in the presence or absence of pretreatment with 200 μM NaHS and/or 2.5 mM PAG for 30 min. (A) NaHS reduces the accumulation of caspase-1 in THP-1 macrophages treated by ox-LDL or ox-LDL + PAG. Immunofluorescent staining of caspase-1 accumulation. Magnification: 200 x. Scale bar, 50 μm. n=3. (B) AFI of active caspase-1 was calculated using Image J software, and represented as fold-change in AFI compared with the control. Fold-change in AFI of the control was normalised to 1. (C) NaHS inhibits the activity of caspase-1 in THP-1 macrophages treated by ox-LDL or ox-LDL + PAG. Quantification of caspase-1 activity in THP-1 cells. Caspase-1 activity was represented as fold-change in activity compared with the control. Fold-change in caspase-1 activity of the control was normalised to 1. n=5. **P<0.01 vs. control, $^{\#}$P<0.05, $^{\#\#}$P<0.01 vs. ox-LDL and $^{\&\&}$P<0.01 vs. ox-LDL + PAG. ox-LDL, oxidized low-density lipoprotein; PMA, phorbol-12-myristate-13-acetate; PAG, D,L-propargylglycine; AFI, average fluorescence intensity.

Immunofluorescence microscopy demonstrated that ox-LDL significantly increased the fluorescence intensity of active caspase-1 in THP-1 cells (Fig. 4A and B) compared with the control. Co-treatment of PAG with ox-LDL significantly increased the fluorescence intensity of caspase-1 compared with ox-LDL alone, whereas PAG treatment alone had no significant impact on the fluorescence intensity of active caspase-1 compared with the control. However, fluorescence intensity of cleaved caspase-1 in THP-1 cells from the ox-LDL + NaHS group significantly decreased compared with the ox-LDL group (Fig. 4A and B). Fluorescence intensity of caspase-1 in the ox-LDL + PAG + NaHS group was significantly lower compared with the ox-LDL+ PAG group (Fig. 4A and B).

Likewise, ox-LDL significantly increased caspase-1 activity in THP-1 cells compared with the control (Fig. 4C). Furthermore, caspase-1 activity of the ox-LDL + PAG group was significantly higher compared with the ox-LDL group (Fig. 4C) while NaHS pretreatment significantly decreased caspase-1 activity compared with the ox-LDL group (Fig. 4C). ox-LDL + PAG + NaHS group had a significantly lower caspase-1 activity compared with ox-LDL + PAG (Fig. 4C).

Moreover, the LPS + ATP-induced increase in caspase-1 activity was also significantly decreased by NaHS pretreatment (Fig. S3), while treatment with PAG (Fig. 4C) or NaHS (Fig. S3) alone did not significantly affect caspase-1 activity. These results suggested that H_2S signaling ameliorated ox-LDL-induced pyroptosis in THP-1 macrophages by suppressing active caspase-1 generation and activity of caspase-1.

H_2S signaling inhibits ox-LDL- and LPS + ATP-induced activation of the canonical pyroptosis signaling pathway. To further assess the effect of endogenous H_2S signaling or exogenous H_2S donors on the canonical pyroptosis signaling pathway. In the present study western blotting assessed the protein expression of canonical pyroptosis specific markers following treatment of THP-1 cells with ox-LDL with or without pretreatment with NaHS or PAG. Treatment with ox-LDL alone significantly increased protein expression levels

of NLRP3, GSDMD, GSDMD-N, pro-caspase-1, caspase-1 and IL-18 compared with the control. ox-LDL + PAG treatment significantly increased protein expression levels of NLRP3, GSDMD-N, caspase-1 and IL-18 compared with the ox-LDL group (Fig. 5). However, NaHS (Fig. S4) or PAG alone (Fig. 5) did not significantly promote protein expression of pyroptosis specific markers in THP-1 cells, and ox-LDL + PAG treatment did not significantly increase GSDMD expression compared with ox-LDL treatment alone (Fig. 5).

Pretreatment with NaHS significantly attenuated the protein expressions of pyroptosis specific markers (NLRP3, GSDMD, GSDMD-N, caspase-1 and IL-18) induced by ox-LDL, ox-LDL + PAG and LPS + ATP in THP-1 cells compared with the ox-LDL group, ox-LDL + PAG group and LPS + ATP group, respectively (Figs. 5 and S4). Moreover, pretreatment with NaHS did not affect pro-caspase-1 expression (Fig. 5A and E) in the ox-LDL + PAG + NaHS group compared with the ox-LDL + PAG group.

To evaluate the impact of H_2S signaling on the pyroptosis pathway activation, ELISA was used to assess the concentrations of NLRP3 in THP-1 cell extract, and IL-1β and IL-18 secretion in cell-free media. ox-LDL and ox-LDL + PAG significantly increased the levels of NLRP3 in THP-1 cell extract and IL-1β and IL-18 in cell culture supernatants compared with the control and ox-LDL groups, respectively (Fig. 6). NaHS pretreatment significantly decreased levels of NLRP3 in THP-1 cell extract and IL-1β and IL-18 secretion induced by ox-LDL and ox-LDL + PAG in the cell culture supernatant compared with the ox-LDL and ox-LDL + PAG groups, respectively (Fig. 6). However, no significant change in IL-1β levels was demonstrated in the PAG compared with the control group (Fig. 6B). Notably, PAG alone increased the levels of NLRP3 in THP-1 cell extract and IL-18 secretion in the cell-free media (Fig. 6A and C).

H_2S inhibits activity of caspase-1 and reduces ox-LDL-induced caspase-1 dependent pyroptosis via S-sulfhydration of pro-caspase-1. S-sulfhydration is the H_2S mediated post-translational modification (58,59) that regulates the structure and functionality of proteins (60). To evaluate whether H_2S mediated S-sulfhydration affects caspase-1 mediated pyroptosis, the level of sulfhydrated pro-caspase-1, release of caspase-1 and IL-1β and caspase-1 activity were measured in THP-1 cells treated with ox-LDL and DTT(S-sulfhydration modification remover) in the presence or absence of NaHS pretreatment. In the control group, pro-caspase-1 underwent S-sulfhydration even in the absence of exogenous H_2S. Moreover, treatment with NaHS alone for 2 h increased the relative levels of pro-caspase-1 S-sulfhydration in THP-1 cells compared with the control group (Fig. 7A and C). By contrast, incubation with DTT induced a significant reduction in the S-sulfhydration levels of pro-caspase-1 in THP-1 cells treated with DTT or DTT + NaHS compared with the control group and the NaHS group, respectively (Fig. 7A and C).

Consistent with these observations, NaHS treatment alone notably decreased activity of caspase-1, whereas treatment with DTT significantly increased caspase-1 activity compared with the control. Likewise, the DTT + NaHS significantly increased caspase-1 activity compared with the NaHS group (Fig. 7D). These results suggest that H_2S may inhibit caspase-1 activity via S-sulfhydration of caspase-1. Furthermore, it was demonstrated that ox-LDL significantly decreased S-sulfhydration of pro-caspase-1 in THP-1 cells (Fig. 7B and E), and increased levels of secreted active caspase-1 (Fig. 7F) and IL-1β (Fig. 7G) in the culture media when compared with THP-1 cells and the culture media of the control group. Similarly, LPS + ATP induced increase in the levels of caspase-1 and IL-1β in cell culture supernatants (Fig. S5). However, NaHS pretreatment restored the decreased S-sulfhydration of pro-caspase-1 induced by ox-LDL with significantly increased levels of S-sulfhydrated pro-caspase-1 compared with the ox-LDL group (Fig. 7B and E). ox-LDL + NaHS group and LPS + ATP + NaHS group had decreased levels of secreted caspase-1 and IL-1β (Figs. S5, 7F and G) when compared with the culture media of the ox-LDL group or LPS + ATP group, while NaHS treatment alone did not increase the levels of secreted caspase-1 and IL-1β (Fig. S5).

Discussion

Although previous studies have reported the role of H_2S in countering inflammation and pyroptosis (40-43,45,54-56,61), the specific molecular mechanisms by which H_2S regulates the pyroptosis signaling pathway and inhibits macrophage pyroptosis are largely unknown. The present study demonstrated a molecular mechanism by which H_2S signaling directly regulates caspase-1-dependent macrophage pyroptosis via S-sulfhydration of pro-caspase-1. To the best of our knowledge, this mechanism has not been previously identified. ox-LDL was demonstrated to significantly decrease S-sulfhydration of pro-caspase-1 by inhibiting endogenous H_2S production, consequently inducing pyroptosis in THP-1 macrophages. This induction occurs via activation of the canonical pyroptosis signaling pathway as well as an increase in enzymatic activity of caspase-1, as reported by previous studies (6,13,32,45). Inhibition of endogenous H_2S production by PAG enhanced ox-LDL-induced expression and activity of pyroptosis-associated proteins, leading to pyroptotic death in macrophages. The exogenous H_2S donor NaHS not only ameliorated ox-LDL-induced macrophage pyroptosis but also mitigated the effect of co-treatment with PAG and ox-LDL on pyroptosis. Finally, decreased levels of pro-caspase-1 S-sulfhydration by DTT or ox-LDL increased caspase-1 activity and secretion of pyroptosis-related proteins (caspase-1, IL-1β and IL-18). Conversely, increased S-sulfhydration of pro-caspase-1 mediated by H_2S decreased caspase-1 activity and secretion of pyroptosis-related proteins (caspase-1, IL-1β and IL-18). These findings, in conjunction with a previous study (45), provide evidence that pro-caspase-1 was a target of H_2S-mediated S-sulfhydration in the modulation of pyroptosis. The present study also demonstrated the role of H_2S-induced S-sulfhydration in the canonical pyroptosis signaling pathway. These findings increase understanding of the molecular mechanisms through which H_2S exerts anti-inflammatory and anti-pyroptotic effects. Furthermore, the findings of the present study establish a foundation for the development of novel H_2S-releasing drugs and anti-atherosclerotic agents targeting the pyroptosis signaling pathway.

Previous studies (1,2,4,6,8,11,13,23) suggest that both excessive pyroptosis in macrophages and release of

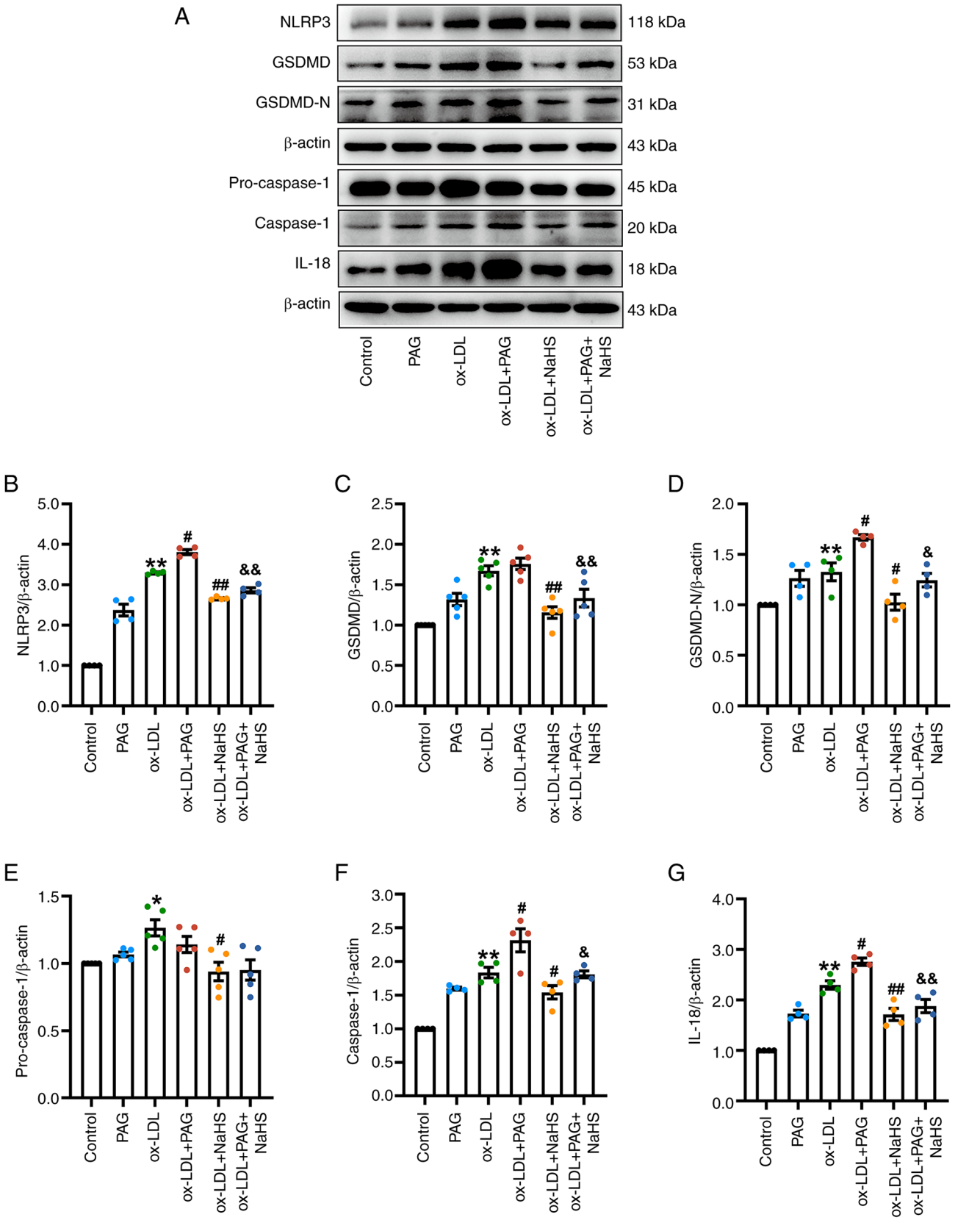

Figure 5. H_2S signaling inhibits ox-LDL-induced activation of the canonical pyroptotic pathway. Immunoblotting was performed to determine the protein levels of NLRP3, pro-caspase-1, caspase-1, GSDMD, GSDMD-N and IL-18 in THP-1 macrophages treated with 100 μg/ml ox-LDL for 23.5 h in the presence or absence of pretreatment with 200 μM NaHS and/or 2.5 mM PAG for 30 min. (A) NaHS reduces the expression of pyroptosis specific markers in THP-1 macrophages treated by ox-LDL or ox-LDL + PAG. Representative immunoblots of pyroptotic indicators in the extracts of THP-1 cells. β-actin served as an internal reference protein. The relative protein levels were quantified based on band intensity. The relative IOD of (B) NLRP3 (n=4), (C) GSDMD (n=5), (D) GSDMD-N (n=4), (E) pro-caspase-1 (n=5), (F) caspase-1 and (G) IL-18 (both n=4) was examined using Image J software. The relative expression levels of these pyroptotic proteins in control group were normalized to 1. *P<0.05, **P<0.01 vs. control, $^{\#}$P<0.05, $^{\#\#}$P<0.01 vs. ox-LDL, $^{\&}$P<0.05 and $^{\&\&}$P<0.01 vs. ox-LDL + PAG. NLRP3, nucleotide-binding oligomerization domain-like receptor family pyrin domain containing 3; GSDMD-N, N-terminal fragment of gasdermin D; ox-LDL, oxidized low-density lipoprotein; PAG, D,L-propargylglycine; IOD, integrated optical density.

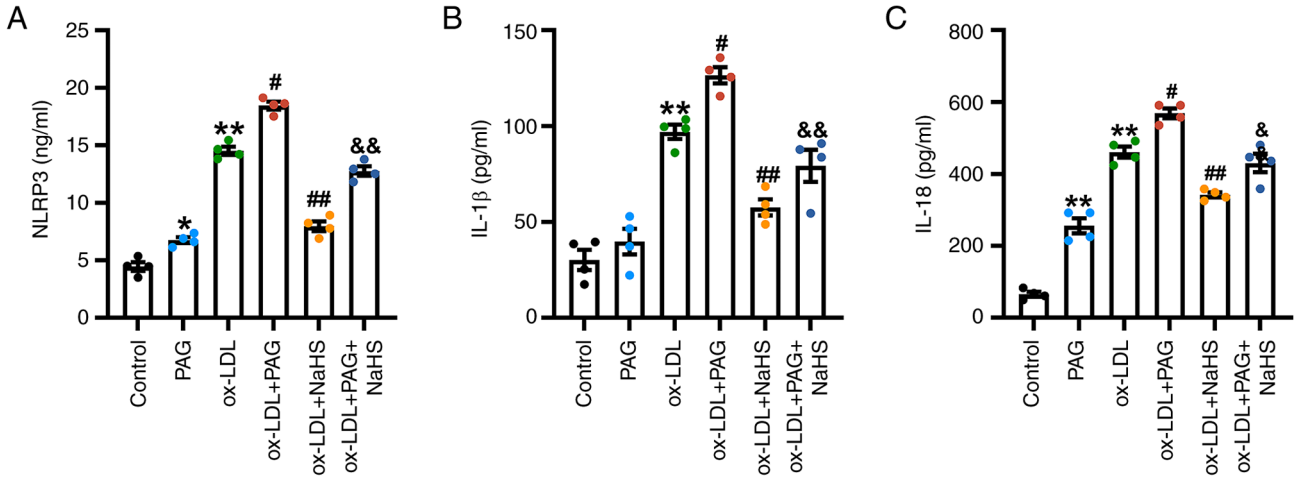

Figure 6. H_2S signaling inhibits ox-LDL-induced generation of pyroptosis-associated NLRP3 and pro-inflammatory cytokines. Following pretreatment for 30 min with 200 μM NaHS and/or 2.5 mM PAG, differentiated THP-1 macrophages were stimulated for 23.5 h with 100 μg/ml ox-LDL. ELISA was performed to quantify levels of (A) NLRP3 in THP-1 cell lysates and (B) IL-1β and (C) IL-18 secretion in cell-free culture medium. n=4. *P<0.05, **P<0.01 vs. control, $^{\#}$P<0.05, $^{\#\#}$P<0.01 vs. ox-LDL and $^{\&}$P<0.05, $^{\&\&}$P<0.01 vs. ox-LDL + PAG. PAG, D,L-propargylglycine; ox-LDL, oxidized low-density lipoprotein; NLRP3, nucleotide-binding oligomerization domain-like receptor family pyrin domain containing 3.

pro-inflammatory molecules by pyroptotic macrophages contribute to the progression of AS. This process enlarges the size of the necrotic lipid core in atherosclerotic plaque, increases plaque instability and increases the risk of arterial thrombosis (4,25,62,63). ox-LDL is an independent pathogenic factor associated with inflammatory responses and AS. ox-LDL has been reported to activate the NLRP3 inflammasome and caspase-1 in macrophages (8,14,32). Activated caspase-1 triggers pyroptosis by directly cleaving GSDMD, inducing development of GSDMD-N formed cell membrane pores and cleaving precursors of IL-1β and IL-18 into active forms (8,13,14,32). Pro-inflammatory cytokines IL-1β and IL-18 are secreted during pyroptosis via GSDMD-N membrane pores, and NLRP3 inflammasome or caspase-1 activation is linked to the maturation and release of these cytokines (1,4,8,11,13,14). During pyroptosis, the plasma membrane is damaged, allowing water influx causing cell swelling, osmotic lysis and release of intracellular contents including pro-inflammatory mediators and LDH, a hallmark of pyroptosis, into the extracellular space (13,54).

The present study demonstrated that ox-LDL decreased cell viability and induced pyroptotic cell death, marked by pronounced cell swelling, membrane rupture and formation of balloon-shaped bubbles extending from the plasma membrane. ox-LDL also increased proportion of PI-stained cells, LDH activity and the protein expression of NLRP3, caspase-1, GSDMD, GSDMD-N, IL-1β and IL-18, which are related to the pyroptosis pathway in THP-1 cells. Moreover, ox-LDL could promote the secretion of pyroptosis-associated cytokines (IL-1β and IL-18) were secreted in cell-free culture supernatant. The aforementioned results are in line with a previous study that showed differentiated THP-1 macrophages can be stimulated to undergo increased pyroptosis by ox-LDL at different ox-LDL concentrations (50, 100 and 150 μg/ml) (45), suggesting that ox-LDL can induce macrophage pyroptosis. Numerous studies have reported increased expression of caspase-1 in lesion macrophages in animal and human AS and in macrophages stimulated by atherosclerotic risk factors (1,9,22,24,42). This implies that caspase-1 is involved in formation of atherosclerotic lesions mediated by macrophage pyroptosis. Consistent with these studies, the present study also demonstrated that ox-LDL increased caspase-1 activity in macrophages. Furthermore, increasing evidence indicates that specific pharmacological inhibition or genetic knockout of caspase-1 decreases macrophage pyroptosis induced by AS-associated risk factors (ox-LDL, homocysteine and cholesterol) and plaque development in $ApoE^{-/-}$ mice (22,24,26-28,31). Therefore, inhibiting the caspase-1-dependent pyroptosis signaling pathway and decreasing macrophage pyroptosis are promising therapeutic strategies for the treatment of AS.

Studies have reported the involvement of H_2S in numerous physiological processes such as lipid metabolism, blood vessel relaxation, blood pressure regulation and neurotransmission (34,36,64,65). H_2S exhibits potent anti-inflammatory properties in numerous types of inflammatory and immune disease including atherosclerosis, multiple sclerosis, inflammatory bowel diseases, ulcerative colitis, asthma and sepsis-induced cardiomyopathy (38,40,41,66-68). In particular, the anti-inflammatory properties of H_2S are associated with its anti-pyroptotic effects (40-43,55,68,69). Administration or pretreatment with exogenous H_2S donors such as GYY4137 and NaHS have been reported to alleviate inflammatory responses by suppressing activation of the NLRP3 inflammasome and the caspase-1-dependent canonical pyroptosis pathway in numerous types of cell (40-43,45,55,68-72). This causes a significant decrease in the inflammation of tissues and organ damage induced by numerous pro-inflammatory pathological factors (40-43,54-56,66,68,69). However, the aforementioned studies have not demonstrated the mechanism by which H_2S inhibits macrophage pyroptosis. The present study demonstrated that exogenous H_2S can inhibit the expression and secretion of pyroptosis-specific markers (NLRP3, caspase-1, GSDMD, GSDMD-N, IL-1β and IL-18), and caspase-1 activity in response to ox-LDL treatment, thereby attenuating morphological and biochemical changes associated with macrophage

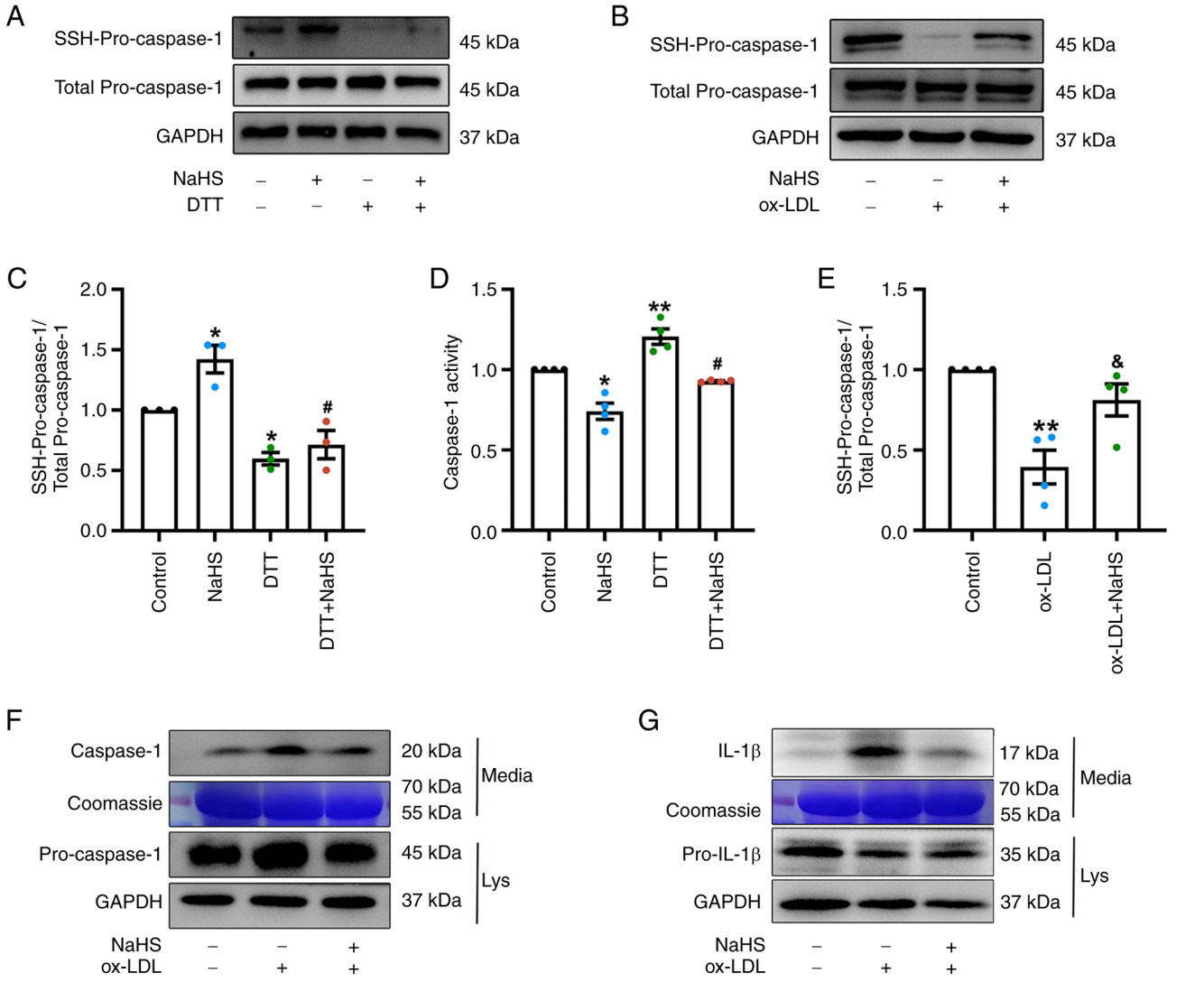

Figure 7. H_2S S-sulfhydrated pro-caspase-1 decreases activity of caspase-1 and ox-LDL-induced pyroptosis. (A) The effect of H_2S and DTT on S-sulfhydration of pro-caspase-1 in THP-1 cells. Biotin switch assay and western blotting were used to assess S-sulfhydration of pro-caspase-1 in THP-1 cells treated with or without 200 μM NaHS for 2 h or 1 mM DTT for 1.5 h, in the presence or absence of pretreatment with 200 μM NaHS for 30 min. DTT served as a negative desulfhydration control. Total pro-caspase-1 and GAPDH were used as loading controls. (B) H_2S increases S-sulfhydration of pro-caspase-1 in ox-LDL stimulated THP-1 cells. THP-1 cells exposed to 100 μg/ml ox-LDL for 23.5 h in the presence or absence of pretreatment with 200 μM NaHS for 30 min. The detection of S-sulfhydration of pro-caspase-1 was performed using biotin switch assay and western blotting. Total pro-caspase-1 and GAPDH were used as loading controls. (C) Quantification of S-sulfhydration of pro-caspase-1 by biotin switch assay in THP-1 cells exposed to treated with or without 200 μM NaHS or/and 1 mM DTT. The protein bands corresponding to S-sulfhydrated pro-caspase-1 were quantified and normalized against those of the total pro-caspase-1 protein. The level of S-sulfhydration of pro-caspase-1 in control group were normalised to 1. n=3. (D) The effect of H_2S and DTT on the activity of caspase-1 in THP-1 macrophages. THP-1 cells were treated with or without 200 μM NaHS for 2 h or 1 mM DTT for 1.5 h, in the presence or absence of pretreatment with 200 μM NaHS for 30 min. Caspase-1 activity assay kit was used to quantify caspase-1 activity in THP-1 cells. Caspase-1 activity was represented as fold-change in activity compared with the control. Fold-change in caspase-1 activity of the control was normalised to 1. n=4. (E) Quantification of S-sulfhydration of pro-caspase-1 by biotin switch assay in THP-1 cells exposed to treated with 100 μg/ml ox-LDL for 23.5 h in the presence or absence of pretreatment with 200 μM NaHS for 30 min. The relative levels of S-sulfhydrated pro-caspase-1 were quantified and normalized to the total pro-caspase-1 protein. The level of S-sulfhydration of pro-caspase-1 in control group were normalised to 1. n=4. (F and G) H_2S reduces the levels of secreted caspase-1 (F) and IL-1β (G) from ox-LDL stimulated THP-1 cells. Western blotting of the precursor and active forms of caspase-1 and IL-1β. n=4. GAPDH in cell lysates and Coomassie brilliant blue staining from total secreted protein in cell-free media were used as loading controls (48,49). *P<0.05, **P<0.01 vs. control, $^{\#}$P<0.05 vs. NaHS; $^{\&}$P<0. 05 vs. ox-LDL. ox-LDL, oxidized low-density lipoprotein; DTT, dithiothreitol; Lys, lysate.

pyroptosis induced by ox-LDL. Therefore, exogenous H_2S exerts both anti-inflammatory and anti-pyroptotic effects.

Furthermore, the present study demonstrated that inhibition of endogenous H_2S production increases the pro-pyroptotic effects of ox-LDL in macrophages by increasing activation of the canonical pyroptosis signaling pathway. Thus, the results of the present study align with previous research demonstrating the anti-pyroptotic effects of H_2S in countering NLRP3/caspase-1/GSDMD-mediated pyroptosis in cellular and mammalian models of acute or chronic inflammation (40,70). As Yue *et al* (71) and Zheng *et al* (72) reported, a potential link may exist between H_2S metabolism and AS via the NLRP3/caspase-1/IL-1β signaling pathway. Zheng *et al* (72) reported that increased activation of caspase-1 and expression of NLRP3 and mature IL-1β in endothelial cells, induced by high glucose + ox-LDL stimulation, is reversed by the addition

of exogenous H_2S. Furthermore, the present study suggested that the effects of H_2S against ox-LDL-induced macrophage pyroptosis were mediated through the inhibition of the NLRP3/caspase-1/GSDMD-dependent canonical pyroptosis signaling pathway. Moreover, the effects of NaHS treatment alone on macrophage pyroptosis were assessed in the present study, which demonstrated that NaHS (200 μM) treatment alone under the same concentration did not significantly promote pyroptosis specific proteins and (NLRP3, GSDMD and GSDMD-N) pyroptosis of THP-1-derived macrophages, while LPS + ATP-induced macrophage pyroptosis was attenuated by NaHS pretreatment. Cell viability assays in the present and a previous study (45) also demonstrated that NaHS treatment alone has no adverse effect on THP-1 macrophages and increased concentrations (50, 100 and 200 μM;) of NaHS significantly reduced ox-LDL-induced pyroptosis in THP-1-derived macrophages. Based on these results, it is suggested that NaHS administration alleviated pyroptosis in ox-LDL-stimulated THP-1 macrophages by inhibiting the activation of the canonical pyroptotic pathway, which exhibited a positive correlation with increased levels of H_2S in THP-1 macrophages.

The dysfunction of H_2S signaling is implicated in development of AS and is associated with ox-LDL-induced macrophage inflammation (38,51,73). In mammalian tissue, H_2S is primarily synthesized endogenously by three key enzymes, CSE, 3-mercaptopyruvate sulfur transferase and cystathionine β-synthetase (CBS), using L-cysteine and homocysteine as primary substrates (34,67). However, the expression and distribution of these three enzymes are tissue- and cell-specific (52). CSE is the main enzyme involved in endogenous H_2S production in multiple types of macrophage (42,51,52). Previous studies also suggest that by suppressing expression and function of CSE and CBS, ox-LDL attenuates production of H_2S in THP-1 cells as well as Raw264.7 macrophages (51,73). ox-LDL can induce DNA hypermethylation of the CSE promoter in macrophages, resulting in suppression of H_2S production and CSE transcription, thereby exacerbating inflammatory responses (74). CSE deficiency or inhibition induces NLRP3 inflammasome activation in inflammatory cellular and mouse models with peritonitis, acute kidney injury, high choline-induced cardiac dysfunction, diabetic cardiomyopathy and colitis (40,70,75-77). Therefore, the present study investigated the impact of endogenous and exogenous H_2S on macrophage pyroptosis following ox-LDL stimulation. The experiment in Fig. 1D assessed the alterations in endogenous H_2S levels in macrophages treated with numerous drugs. It was demonstrated that ox-LDL and/or PAG decreased H_2S synthesis by inhibiting CSE, while NaHS increased H_2S levels in ox-LDL- and/or PAG-treated THP-1 cells, consistent with previous findings (51). Notably, inhibiting endogenous generation of H_2S with PAG promoted pyroptosis in ox-LDL-stimulated THP-1 macrophages by exacerbating the activation of the pyroptosis signaling pathway. This was observed through morphological changes associated with pyroptosis, increased PI-positive cell counts, LDH release, accumulation of cleaved caspase-1, caspase-1 activity and upregulation of pyroptosis-related proteins in THP-1 cells, compared with those stimulated by ox-LDL alone. This exacerbation of pyroptotic effects by co-treatment with PAG with ox-LDL was attenuated by pretreatment with NaHS.

Numerous studies have reported that CSE deficiency/silencing/inhibition by PAG in monosodium urate and dextran sulphate sodium stimulated bone marrow-derived macrophages, THP-1 cells, RAW264.7 cells murine peritoneal macrophages stimulated with LPS (40,71,77-79) increase the protein expression levels of NLRP3, active caspase-1, GSDMD and IL-1β, which are associated with the pyroptosis pathway. Conversely, treatment with exogenous H_2S donors can suppress expression of NLRP3, GSDMD-N, cleaved caspase-1 and IL-1β in CSE-deficient mice and macrophages (40,77,79). These findings align with the present study, demonstrating that the suppression of endogenous H_2S production by PAG exacerbated the pro-pyroptotic role of ox-LDL in macrophages derived from THP-1, while supplementation with exogenous H_2S via NaHS inhibited macrophage pyroptosis by downregulating the canonical pyroptosis pathway. This suggests that H_2S signaling served an anti-pyroptotic role in ox-LDL-induced macrophage inflammation. Moreover, endogenously produced H_2S by CSE may be a critical negative regulator of the canonical pyroptosis pathway.

Although increasing evidence suggests a role for H_2S signaling in the inhibition of NLRP3 inflammasome activation and caspase-1-dependent canonical pyroptosis (40-43,45,54-56,61), there is a lack of understanding regarding the molecular mechanisms by which H_2S signaling inhibits macrophage pyroptosis. H_2S-mediated protein post-translational modification targeting sulfhydryl groups, also known as S-sulfhydration, is a key molecular mechanism by which H_2S regulates structure and function of target proteins (34,44,60). Numerous target proteins undergo S-sulfhydration and there is growing evidence that these proteins are involved in anti-inflammatory responses and anti-atherosclerotic effects (34,42,59,73,80). A previous study reported that by S-sulfhydrating c-Jun in THP-1 macrophages, H_2S decreases activation of the NLRP3 inflammasome induced by H_2O_2 (42). However, to date there is no direct evidence for H_2S mediated S-sulfhydration directly regulates pyroptosis specific proteins in the protection against macrophage pyroptosis.

Caspase-1 and caspase-3 both belong to the caspase family; activated caspase-3 can induce macrophage pyroptosis by cleaving GSDME, a member of the gasdermin family, into GSDME-N (2,16). Pro-caspase-3 is constitutively S-sulfhydrated in unstimulated cells and H_2S can inhibit activity of caspase-3 and cell apoptosis by enhancing the S-sulfhydration levels of caspase-3 (60,64). Based on these findings, along with the suppressive effects of H_2S on caspase-1 activity and accumulation demonstrated in the present study, it was hypothesized that caspase-1 serves as a target protein for H_2S-mediated S-sulfhydration and that H_2S inhibits activation or activity of caspase-1 and macrophage pyroptosis through the S-sulfhydration of caspase-1. To validate this hypothesis, the desulfhydration reagent DTT and NaHS were used to assess the effect of S-sulfhydration induced by H_2S on caspase-1 activity. The biotin switch assay used is an internationally recognized measurement technique for detecting protein S-sulfhydration (34,44,50). Specifically, the results demonstrated the existence of basal S-sulfhydrated

pro-caspase-1. S-sulfhydration of pro-caspase-1 was increased following treatment with NaHS, resulting in a notable decrease in the activity of caspase-1 in NaHS treated THP-1 cells. Notably, both the basal S-sulfhydration of pro-caspase-1 and the NaHS-induced S-sulfhydration of pro-caspase-1 were significantly decreased by the desulfhydration reagent DTT, which increased caspase-1 activity or mitigated the inhibitory effect of NaHS on caspase-1 activity in macrophages. These findings suggested that H_2S-induced suppression of caspase-1 activity and macrophage pyroptosis may be attributed to reversible S-sulfhydration of protein thiols within pro-caspase-1.

To validate the inhibitory effects of H_2S-mediated caspase-1 S-sulfhydration on macrophage pyroptosis induced by ox-LDL, the impact of the S-sulfhydration of pro-caspase-1 on pyroptosis-induced secretion of caspase-1 and IL-1β, mediated by GSDMD-N-formed membrane pores in THP-1 cells exposed to ox-LDL was assessed. This demonstrated a notable reduction in the basal S-sulfhydration of pro-caspase-1 in THP-1 cells treated with ox-LDL. Attenuation of S-sulfhydration of pro-caspase-1 induced by ox-LDL was mitigated by NaHS pretreatment. Meanwhile, NaHS pretreatment could reduce macrophage pyroptosis-induced secretion of activated caspase-1 and mature IL-1β. Therefore, these results suggested that pro-caspase-1 can be S-sulfhydrated by H_2S, which inhibited the generation of active caspase-1, and led to the deactivation of downstream pyroptotic signaling pathways. The present study demonstrated that ox-LDL can induce inflammation-mediated macrophage pyroptosis by upregulating the NLRP3/caspase-1/GSDMD-dependent canonical pyroptosis signaling pathway. ox-LDL can also inhibit endogenous H_2S synthesis, thereby diminishing the anti-inflammatory and anti-pyroptotic effects of endogenous H_2S by decreasing the constitutive S-sulfhydration of pro-caspase-1 mediated by endogenous H_2S, leading to increased caspase-1 activity and activation of the caspase-1-dependent pyroptosis pathway. By contrast, pretreatment with exogenous H_2S increased intracellular H_2S concentrations, thereby exerting an anti-pyroptotic effect by directly inhibiting ox-LDL-induced activation of the NLRP3/caspase-1/GSDMD axis. The increased intracellular H_2S resulting from exogenous H_2S pretreatment increased the S-sulfhydration of pro-caspase-1. It was plausible to hypothesize that H_2S inhibits caspase-1 activity by S-sulfhydrating pro-caspase-1, thereby preventing cleavage of GSDMD/IL-1β, and decreasing macrophage pyroptosis.

There are several limitations to the present study. First, only the function of the CSE/H_2S pathway in pyroptosis of macrophages was assessed. However, as the downregulated endogenous CBS/H_2S pathway is implicated in ox-LDL-induced macrophage inflammation (73), further study is required to elucidate the role of the CBS/H_2S pathway in preventing macrophage pyroptosis. Second, the present study did not identify specific residues that are S-sulfhydrated in pro-caspase-1. Although the present study represented a preliminary investigation of the relationship between S-sulfhydration of pro-caspase-1 and canonical caspase-1-dependent pyroptosis, before implementing it, it would be profitable to identify the specific or crucial cysteine residues in caspase-1 that are S-sulfhydrated. Liquid chromatography with tandem mass spectrometry can determine post-translational modifications

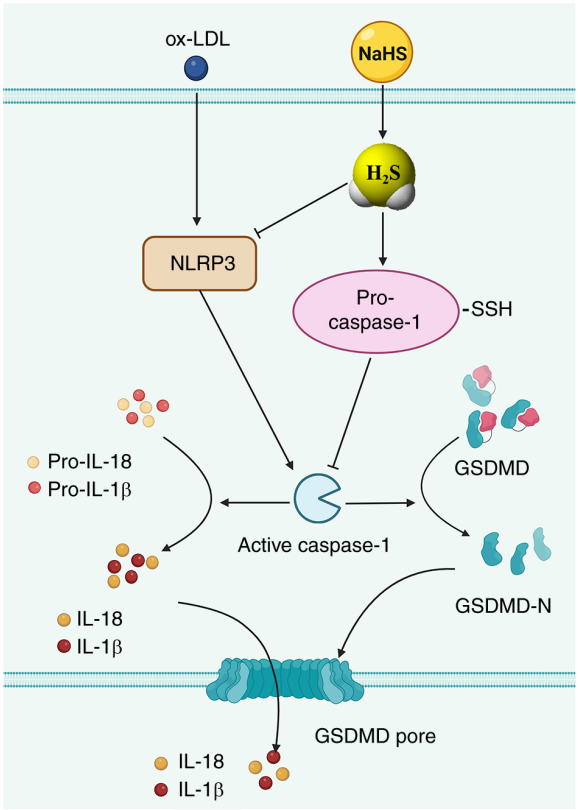

Figure 8. Potential mechanism by which H_2S inhibits ox-LDL-induced pyroptosis in macrophages. ox-LDL activates the NLRP3 inflammasome, increasing caspase-1 activation/activity, partially via a decrease in S-sulfhydration of pro-caspase-1. This cascade promotes GSDMD cleavage, resulting in formation of membrane pores and the release of pro-inflammatory cytokines from GSDMD-N-formed membrane pores to induce pyroptosis in macrophages. Exogenous H_2S treatment can suppress NLRP3 inflammasome activation and decrease activation/activity of caspase-1 by enhancing S-sulfhydration of pro-caspase-1. This decreases production of GSDMD-N and the release of activated caspase-1 and mature pro-inflammatory cytokines via GSDMD-N formed membrane pores, ultimately decreasing ox-LDL-induced macrophage pyroptosis. ox-LDL, oxidized low-density lipoprotein; NLRP3, nucleotide-binding oligomerization domain-like receptor family pyrin domain containing 3; GSDMD-N, N-terminal fragment of gasdermin D.

of proteins; to the best of our knowledge, however, there are few studies (50,64,81) detecting the specific cysteine sites of S-sulfhydration modification using mass spectrometry due to this technique has a propensity to identify false positive cysteine sites (82,83). Therefore, mass spectrometry results identifying S-sulfhydrated Cys in pro-caspase-1 would require verification through mutation studies to exclude the possibility of false positive S-sulfhydrated sites (84,85). In future studies, these techniques should be used to identify the key Cys residues that are S-sulfhydrated in pro-caspase-1. Likewise, mutation studies should be used to clarify the specific effects of Cys site, as well as potential synergistic effects of multiple Cys site mutations on bioactivity of caspase-1 and the interactions between NLRP3/caspase-1/GSDMD signaling and macrophage pyroptosis.

Previous studies (86,87) have reported key interplay and competition between nitric oxide-induced S-nitrosylation and H_2S-induced S-sulfhydration. These post-translational modifications can occur at the same Cys residues of target proteins but exert opposing effects. This suggests that these

post-translational modifications may maintain normal function of target proteins (44,82). Additional studies are required to assess the S-nitrosylation status of pro-caspase-1 under normal conditions and in response to pro-inflammatory stimuli. Moreover, the role of homeostasis between S-nitrosylation and S-sulfhydration of caspase-1 at key Cys sites in macrophage pyroptosis warrants further investigation. Lastly, in addition to modulating the function and activity of target proteins, S-sulfhydration can also regulate subcellular localization, protein-protein interactions and protein stability. Thus, immunoprecipitation experiments should be performed to assess how S-nitrosylation and S-sulfhydration at different Cys residues of caspase-1 affects interactions with other pyroptosis-specific proteins.

In conclusion, it was hypothesized that endogenous pro-caspase-1 undergoes constitutive S-sulfhydration in macrophages under normal conditions. Furthermore, decreased generation of H_2S triggered by ox-LDL stimulation in macrophages decreases basal S-sulfhydration of pro-caspase-1. This increases the activation of caspase-1, thereby initiating a downstream events in the caspase-1-dependent canonical pyroptosis, including GSDMD cleavage, GSDMD-N-mediated development of membrane pores and release of activated caspase-1 and pro-inflammatory cytokines via GSDMD-N membrane pores. Consequently, macrophage pyroptosis is induced (Fig. 8). Finally, the present study demonstrated that exogenous H_2S donors mitigates ox-LDL-induced macrophage pyroptosis by suppressing expression of the NLRP3 inflammasome, the generation of functional caspase-1, caspase-1 activity, production of the pyroptosis executioner (GSDMD-N) and the secretion of mature pro-inflammatory cytokines (IL-1β and IL-18). This mitigation occurs by elevating H_2S levels and S-sulfhydration of pro-caspase-1 (Fig. 8). Such modifications may account for deactivation of downstream signaling pathways associated with caspase-1, including the generation of active caspase-1, the suppression of GSDMD cleavage and formation of membrane pores mediated by GSDMD-N. Furthermore, this leads to a decrease in the release of pro-inflammatory mediators through GSDMD-N-formed membrane pores.

The present study demonstrated a novel molecular mechanism by which H_2S directly regulates the caspase-1-dependent pyroptotic pathway, thereby ameliorating macrophage pyroptosis induced by ox-LDL stimulation. Furthermore, the present results provide novel insights into the involvement of S-sulfhydration in functional regulation of caspase-1. The results of the present study supported the development of novel H_2S-releasing drugs specifically target pyroptosis-specific proteins and the S-sulfhydration of caspase-1.

Acknowledgements

The authors would like to thank Professor Wenjing Xu (Department of Pathology, School of Basic Medical Science, Xi'an Medical University, Xi'an, Shanxi, China.) for technical assistance with biotin switch assay and Miss Yan Wang (Ministry of Education Key Laboratory of Xinjiang Endemic and Ethnic Diseases, Shihezi University, Shihezi, Xinjiang, China) for providing technical assistance with immunofluorescent staining.

Funding

The present study was supported by National Natural Science Foundation of China (grant no. 81600325), Project of Science and Technology Innovation from Xinjiang Production and Construction Corps (grant no. 2022CB002-10), Non-profit Central Research Institute Fund of Chinese Academy of Medical Sciences (grant no. 2020-PT330-003), Open Research Fund of NHC Key Laboratory of Prevention and Treatment of Central Asia High Incidence Diseases (grant no. KF202107) and Science and Technology Project of Shihezi University (grant nos. CXBJ201906 and ZZZC202135).

Availability of data and materials

The data generated in the present study may be requested from the corresponding author.

Authors' contributions

ZJ, XZ, ZL and HY performed H_2S detection, Hoechst 33342/PI double staining, caspase-1 activity measurement, immunofluorescent staining, immunoblotting, ELISA and analyzed/interpreted data. ZJ and XZ conducted biotin switch assay. CL analyzed the data of biotin switch assay. XT and KM analyzed and interpreted data of Hoechst 33342/PI double staining, immunofluorescent staining and ELISA. LZ and LL designed the experiments in this study and drafted/revised the manuscript. ZJ, XZ, LZ and LL confirm the authenticity of all the raw data. All authors have read and approved the final manuscript.

Ethics approval and consent to participate

Not applicable.

Patient consent for publication

Not applicable.

Competing interests

The authors declare that they have no competing interests.

References

1. Xu YJ, Zheng L, Hu YW and Wang Q: Pyroptosis and its relationship to atherosclerosis. Clin Chim Acta 476: 28-37, 2018.
2. Wang Q, Wu J, Zeng Y, Chen K, Wang C, Yang S, Sun N, Chen H, Duan K and Zeng G: Pyroptosis: A pro-inflammatory type of cell death in cardiovascular disease. Clin Chim Acta 510: 62-72, 2020.
3. Miao EA, Rajan JV and Aderem A: Caspase-1-induced pyroptotic cell death. Immunol Rev 243: 206-214, 2011.
4. He X, Fan X, Bai B, Lu N, Zhang S and Zhang L: Pyroptosis is a critical immune-inflammatory response involved in atherosclerosis. Pharmacol Res 165: 105447, 2021.
5. Zychlinsky A, Prevost MC and Sansonetti PJ: Shigella flexneri induces apoptosis in infected macrophages. Nature 358: 167-169, 1992.
6. Peng X, Chen H, Li Y, Huang D, Huang B and Sun D: Effects of NIX-mediated mitophagy on ox-LDL-induced macrophage pyroptosis in atherosclerosis. Cell Biol Int 44: 1481-1490, 2020.

7. Hilbi H, Moss JE, Hersh D, Chen Y, Arondel J, Banerjee S, Flavell RA, Yuan J, Sansonetti PJ and Zychlinsky A: Shigella-induced apoptosis is dependent on caspase-1 which binds to IpaB. J Biol Chem 273: 32895-32900, 1998.
8. He B, Nie Q, Wang F, Han Y, Yang B, Sun M, Fan X, Ye Z, Liu P and Wen J: Role of pyroptosis in atherosclerosis and its therapeutic implications. J Cell Physiol 36: 7159-7175, 2021.
9. Lin L, Zhang MX, Zhang L, Zhang D, Li C and Li YL: Autophagy, pyroptosis, and ferroptosis: New regulatory mechanisms for atherosclerosis. Front Cell Dev Biol 9: 809955, 2022.
10. Liu JR, Wang C, Li J, Yu Y, Liu Y, Liu H, Peng Q and Guan X: Autophagy blockage promotes the pyroptosis of ox-LDL-treated macrophages by modulating the p62/Nrf2/ARE axis. J Physiol Biochem 77: 419-429, 2021.
11. Xu XD, Chen JX, Zhu L, Xu ST, Jiang J and Ren K: The emerging role of pyroptosis-related inflammasome pathway in atherosclerosis. Mol Med 28: 160, 2022.
12. Taabazuing CY, Okondo MC and Bachovchin DA: Pyroptosis and apoptosis pathways engage in bidirectional crosstalk in monocytes and macrophages. Cell Chem Biol 24: 507-514.e4, 2017.
13. Martinet W, Coornaert I, Puylaert P and De Meyer GRY: Macrophage death as a pharmacological target in atherosclerosis. Front Pharmacol 10: 306, 2019.
14. Zeng C, Wang R and Tan H: Role of pyroptosis in cardiovascular diseases and its therapeutic implications. Int J Biol Sci 15: 1345-1357, 2019.
15. Humphries F, Shmuel-Galia L, Ketelut-Carneiro N, Li S, Wang B, Nemmara VV, Wilson R, Jiang Z, Khalighinejad F, Muneeruddin K, *et al*: Succination inactivates gasdermin D and blocks pyroptosis. Science 369: 1633-1637, 2020.
16. Ji N, Qi Z, Wang Y, Yang X, Yan Z, Li M, Ge Q and Zhang J: Pyroptosis: A new regulating mechanism in cardiovascular disease. J Inflamm Res 14: 2647-2666, 2021.
17. Huang SS, Guo DY, Jia BB, Cai GL, Yan J, Lu Y and Yang ZX: Dimethyl itaconate alleviates the pyroptosis of macrophages through oxidative stress. BMC Immunol 22: 72, 2021.
18. Wang K, Sun Q, Zhong X, Zeng M, Zeng H, Shi X, Li Z, Wang Y, Zhao Q, Shao F and Ding J: Structural mechanism for GSDMD targeting by autoprocessed caspases in pyroptosis. Cell 180: 941-955.e20, 2020.
19. Yuan YY, Xie KX, Wang SL and Yuan LW: Inflammatory caspase-related pyroptosis: Mechanism, regulation and therapeutic potential for inflammatory bowel disease. Gastroenterol Rep (Oxf) 6: 167-176, 2018.
20. Jiang M, Sun X, Liu S, Tang Y, Shi Y, Bai Y, Wang Y, Yang Q, Yang Q, Jiang W, *et al*: Caspase-11-gasdermin D-mediated pyroptosis is involved in the pathogenesis of atherosclerosis. Front Pharmacol 12: 657486, 2021.
21. Puylaert P, Van Praet M, Vaes F, Neutel CHG, Roth L, Guns PJ, De Meyer GRY and Martinet W: Gasdermin D deficiency limits the transition of atherosclerotic plaques to an inflammatory phenotype in ApoE knock-out mice. Biomedicines 10: 1171, 2022.
22. Wang R, Wang Y, Mu N, Lou X, Li W, Chen Y, Fan D and Tan H: Activation of NLRP3 inflammasomes contributes to hyperhomocysteinemia-aggravated inflammation and atherosclerosis in apoE-deficient mice. Lab Invest 97: 922-934, 2017.
23. Liu C, Jiang Z, Pan Z and Yang L: The function, regulation and mechanism of programmed cell death of macrophages in atherosclerosis. Front Cell Dev Biol 9: 809516, 2022.
24. Liu S, Tao J, Duan F, Li H and Tan H: HHcy induces pyroptosis and atherosclerosis via the lipid raft-mediated NOX-ROS-NLRP3 inflammasome pathway in apoE$^{-/-}$ mice. Cells 11: 2438, 2022.
25. Zeng Z, Li G, Wu S and Wang Z: Role of pyroptosis in cardiovascular disease. Cell Prolif 52: e12563, 2019.
26. Hendrikx T, Jeurissen MLJ, van Gorp PJ, Gijbels MJ, Walenbergh SMA, Houben T, van Gorp R, Pöttgens CC, Stienstra R, Netea MG, *et al*: Bone marrow-specific caspase-1/11 deficiency inhibits atherosclerosis development in Ldlr(-/-) mice. FEBS J 282: 2327-2338, 2015.
27. Jin Y, Liu Y, Xu L, Xu J, Xiong Y, Peng Y, Ding K, Zheng S, Yang N, Zhang Z, *et al*: Novel role for caspase 1 inhibitor VX765 in suppressing NLRP3 inflammasome assembly and atherosclerosis via promoting mitophagy and efferocytosis. Cell Death Dis 13: 512, 2022.
28. Liu S, Xu DS, Ma JL, Huang P, Wu D and Ren LQ: LncRNA H19 mitigates oxidized low-density lipoprotein induced pyroptosis via caspase-1 in Raw 264.7 Cells. Inflammation 44: 2407-2418, 2021.
29. Opoku E, Traughber CA, Zhang D, Iacano AJ, Khan M, Han J, Smith JD and Gulshan K: Gasdermin D mediates inflammation-induced defects in reverse cholesterol transport and promotes atherosclerosis. Front Cell Dev Biol 9: 715211, 2021.
30. Rathkey JK, Zhao J, Liu Z, Chen Y, Yang J, Kondolf HC, Benson BL, Chirieleison SM, Huang AY, Dubyak GR, *et al*: Chemical disruption of the pyroptotic pore-forming protein gasdermin D inhibits inflammatory cell death and sepsis. Sci Immunol 3: eaat2738, 2018.
31. Westerterp M, Fotakis P, Ouimet M, Bochem AE, Zhang H, Molusky MM, Wang W, Abramowicz S, la Bastide-van Gemert S, Wang N, *et al*: Cholesterol efflux pathways suppress inflammasome activation, NETosis, and atherogenesis. Circulation 138: 898-912, 2018.
32. Zeng W, Wu D, Sun Y, Suo Y, Yu Q, Zeng M, Gao Q, Yu B, Jiang X and Wang Y: The selective NLRP3 inhibitor MCC950 hinders atherosclerosis development by attenuating inflammation and pyroptosis in macrophages. Sci Rep 11: 19305, 2021.
33. Robinson N, Ganesan R, Hegedűs C, Kovács K, Kufer TA and Virág L: Programmed necrotic cell death of macrophages: Focus on pyroptosis, necroptosis, and parthanatos. Redox Biol 26: 101239, 2019.
34. Gupta R, Sahu M, Tripathi R, Ambasta RK and Kumar P: Protein S-sulfhydration: Unraveling the prospective of hydrogen sulfide in the brain, vasculature and neurological manifestations. Ageing Res Rev 76: 101579, 2022.
35. Pang PP, Zhang HY, Zhang DC, Tang JX, Gong Y, Guo YC and Zheng CB: Investigating the impact of protein S-sulfhydration modification on vascular diseases: A comprehensive review. Eur J Pharmacol 966: 176345, 2024.
36. Cirino G, Szabo C and Papapetropoulos A: Physiological roles of hydrogen sulfide in mammalian cells, tissues, and organs. Physiol Rev 103: 31-276, 2023.
37. Bibli SI, Hu J, Leisegang MS, Wittig J, Zukunft S, Kapasakalidi A, Fisslthaler B, Tsilimigras D, Zografos G, Filis K, *et al*: Shear stress regulates cystathionine γ lyase expression to preserve endothelial redox balance and reduce membrane lipid peroxidation. Redox Biol 28: 101379, 2020.
38. Zhang H, Bai Z, Zhu L, Liang Y, Fan X, Li J, Wen H, Shi T, Zhao Q and Wang Z: Hydrogen sulfide donors: Therapeutic potential in anti-atherosclerosis. Eur J Med Chem 205: 112665, 2020.
39. Zhang L, Wang Y, Li Y, Li L, Xu S, Feng X and Liu S: Hydrogen sulfide (H_2S)-releasing compounds: Therapeutic potential in cardiovascular diseases. Front Pharmacol 9: 1066, 2018.
40. Castelblanco M, Lugrin J, Ehirchiou D, Ishii I, So A, Martinon F and Busso N: Hydrogen sulfide inhibits NLRP3 inflammasome activation and reduces cytokine production both in vitro and in a mouse model of inflammation. J Biol Chem 293: 2546-2557, 2018.
41. Li J, Ma J, Li M, Tao J, Chen J, Yao C and Yao S: GYY4137 alleviates sepsis-induced acute lung injury in mice by inhibiting the PDGFRβ/Akt/NF-κB/NLRP3 pathway. Life Sci 271: 119192, 2021.
42. Lin Z, Altaf N, Li C, Chen M, Pan L, Wang D, Xie L, Zheng Y, Fu H, Han Y and Ji Y: Hydrogen sulfide attenuates oxidative stress-induced NLRP3 inflammasome activation via S-sulfhydrating c-Jun at Cys269 in macrophages. Biochim Biophys Acta Mol Basis Dis 1864: 2890-2900, 2018.
43. Luo ZL, Ren JD, Huang Z, Wang T, Xiang K, Cheng L and Tang LJ: The role of exogenous hydrogen sulfide in free fatty acids induced inflammation in macrophages. Cell Physiol Biochem 42: 1635-1644, 2017.
44. Zhang D, Du J, Tang C, Huang Y and Jin H: H_2S-induced sulfhydration: Biological function and detection methodology. Front Pharmacol 8: 608, 2017.
45. Zhang XL, Tian XQ, Jia ZL, Liu BW, Liang GY, Zhang ZC, Li L and Zhang L: Sodium hydrosulfide attenuates pyroptosis of macrophages by inhibiting classical pyroptosis signaling pathway. Chin J Pathophysiol 38: 1015-1023, 2022.
46. Chiu HW, Li LH, Hsieh CY, Rao YK, Chen FH, Chen A, Ka SM and Hua KF: Glucosamine inhibits IL-1β expression by preserving mitochondrial integrity and disrupting assembly of the NLRP3 inflammasome. Sci Rep 9: 5603, 2019.
47. Mayes-Hopfinger L, Enache A, Xie J, Huang CL, Köchl R, Tybulewicz VLJ, Fernandes-Alnemri T and Alnemri ES: Chloride sensing by WNK1 regulates NLRP3 inflammasome activation and pyroptosis. Nat Commun 12: 4546, 2021.
48. Xu G, Fu S, Zhan X, Wang Z, Zhang P, Shi W, Qin N, Chen Y, Wang C, Niu M, *et al*: Echinatin effectively protects against NLRP3 inflammasome-driven diseases by targeting HSP90. JCI Insight 6: e134601, 2021.

49. Chen Y, Li R, Wang Z, Hou X, Wang C, Ai Y, Shi W, Zhan X, Wang JB, Xiao X, *et al*: Dehydrocostus lactone inhibits NLRP3 inflammasome activation by blocking ASC oligomerization and prevents LPS-mediated inflammation in vivo. Cell Immunol 349: 104046, 2020.
50. Mustafa AK, Gadalla MM, Sen N, Kim S, Mu W, Gazi SK, Barrow RK, Yang G, Wang R and Snyder SH: H_2S signals through protein S-sulfhydration. Sci Signal 2: ra72, 2009.
51. Wang XH, Wang F, You SJ, Cao YJ, Cao LD, Han Q, Liu CF and Hu LF: Dysregulation of cystathionine γ-lyase (CSE)/hydrogen sulfide pathway contributes to ox-LDL-induced inflammation in macrophage. Cell Signal 25: 2255-2262, 2013.
52. Zhang H, Du J, Huang Y, Tang C and Jin H: Hydrogen sulfide regulates macrophage function in cardiovascular diseases. Antioxid Redox Signal 38: 45-56, 2023.
53. Hu HJ, Qiu J, Zhang C, Tang ZH, Qu SL and Jiang ZS: Hydrogen sulfide improves ox-LDL-induced expression levels of Lp-PLA_2 in THP-1 monocytes via the p38MAPK pathway. Mol Med Rep 23: 358, 2021.
54. Hu Q, Zhang R, Zheng J, Song M, Gu C and Li W: Hydrogen sulfide attenuates uranium-induced kidney cells pyroptosis via upregulation of PI3K/AKT/mTOR signaling. J Biochem Mol Toxicol 37: e23220, 2023.
55. Wang L, Meng J, Wang C, Wang Y, Yang C and Li Y: Hydrogen sulfide attenuates cigarette smoke-induced pyroptosis through the TLR4/NF-κB signaling pathway. Int J Mol Med 49: 56, 2022.
56. Zhu X, Lu R, Zhang G, Fan L, Zhan Y, Chen G and Zhou L: Diallyl trisulfide attenuates alcohol-induced hepatocyte pyroptosis via elevation of hydrogen sulfide. Biosci Biotechnol Biochem 86: 1552-1561, 2022.
57. Yu J, Cui X, Zhang X, Cheng M and Cui X: Advances in the occurrence of pyroptosis: A novel role in atherosclerosis. Curr Pharm Biotechnol 22: 1548-1558, 2021.
58. Ding Y, Wang H, Geng B and Xu G: Sulfhydration of perilipin 1 is involved in the inhibitory effects of cystathionine gamma lyase/hydrogen sulfide on adipocyte lipolysis. Biochem Biophys Res Commun 521: 786-790, 2020.
59. Xie L, Gu Y, Wen M, Zhao S, Wang W, Ma Y, Meng G, Han Y, Wang Y, Liu G, *et al*: Hydrogen sulfide induces Keap1 S-sulfhydration and suppresses diabetes-accelerated atherosclerosis via Nrf2 activation. Diabetes 65: 3171-3184, 2016.
60. Ye X, Li Y, Lv B, Qiu B, Zhang S, Peng H, Kong W, Tang C, Huang Y, Du J and Jin H: Endogenous hydrogen sulfide persulfidates Caspase-3 at cysteine 163 to inhibit doxorubicin-induced cardiomyocyte apoptosis. Oxid Med Cell Longev 2022: 6153772, 2022.
61. He TT, Zhang XL, Jia ZL, Wang Y, Ma KT, Li L and Zhang L: Hydrogen sulfide inhibits oxidized low-density lipoprotein-induced pyroptosis in vascular endothelial cells by down-regulating NLRP3/caspase-1 signaling pathway. Chin J Pathophysiol 37: 1738-1746, 2021.
62. Qian Z, Zhao Y, Wan C, Deng Y, Zhuang Y, Xu Y, Zhu Y, Lu S and Bao Z: Pyroptosis in the initiation and progression of atherosclerosis. Front Pharmacol 12: 652963, 2021.
63. Yang Z, Shi J, Chen L, Fu C, Shi D and Qu H: Role of pyroptosis and ferroptosis in the progression of atherosclerotic plaques. Front Cell Dev Biol 10: 811196, 2022.
64. Braunstein I, Engelman R, Yitzhaki O, Ziv T, Galardon E and Benhar M: Opposing effects of polysulfides and thioredoxin on apoptosis through caspase persulfidation. J Biol Chem 295: 3590-3600, 2020.
65. Sun F, Luo JH, Yue TT, Wang FX, Yang CL, Zhang S, Wang XQ and Wang CY: The role of hydrogen sulphide signalling in macrophage activation. Immunology 162: 3-10, 2021.
66. Chen Y, Jin S, Teng X, Hu Z, Zhang Z, Qiu X, Tian D and Wu Y: Hydrogen sulfide attenuates LPS-induced acute kidney injury by inhibiting inflammation and oxidative stress. Oxid Med Cell Longev 2018: 6717212, 2018.
67. Dilek N, Papapetropoulos A, Toliver-Kinsky T and Szabo C: Hydrogen sulfide: An endogenous regulator of the immune system. Pharmacol Res 161: 105119, 2020.
68. Zhou T, Qian H, Zheng N, Lu Q and Han Y: GYY4137 ameliorates sepsis-induced cardiomyopathy via NLRP3 pathway. Biochim Biophys Acta Mol Basis Dis 1868: 166497, 2022.
69. Wu D, Zhong P, Wang J and Wang H: Exogenous hydrogen sulfide mitigates LPS + ATP-induced inflammation by inhibiting NLRP3 inflammasome activation and promoting autophagy in L02 cells. Mol Cell Biochem 457: 145-156, 2019.
70. Ni J, Jiang L, Shen G, Xia Z, Zhang L, Xu J, Feng Q, Qu H, Xu F and Li X: Hydrogen sulfide reduces pyroptosis and alleviates ischemia-reperfusion-induced acute kidney injury by inhibiting NLRP3 inflammasome. Life Sci 284: 119466, 2021.
71. Yue LM, Gao YM and Han BH: Evaluation on the effect of hydrogen sulfide on the NLRP3 signaling pathway and its involvement in the pathogenesis of atherosclerosis. J Cell Biochem 120: 481-492, 2019.
72. Zheng Q, Pan L and Ji Y: H_2S protects against diabetes-accelerated atherosclerosis by preventing the activation of NLRP3 inflammasome. J Biomed Res 34: 94-102, 2019.
73. Du J, Huang Y, Yan H, Zhang Q, Zhao M, Zhu M, Liu J, Chen SX, Bu D, Tang C and Jin H: Hydrogen sulfide suppresses oxidized low-density lipoprotein (ox-LDL)-stimulated monocyte chemoattractant protein 1 generation from macrophages via the nuclear factor κB (NF-κB) pathway. J Biol Chem 289: 9741-9753, 2014.
74. Du HP, Li J, You SJ, Wang YL, Wang F, Cao YJ, Hu LF and Liu CF: DNA methylation in cystathionine-γ-lyase (CSE) gene promoter induced by ox-LDL in macrophages and in apoE knockout mice. Biochem Biophys Res Commun 469: 776-782, 2016.
75. Bai L, Dai J, Xia Y, He K, Xue H, Guo Q, Tian D, Xiao L, Zhang X, Teng X, *et al*: Hydrogen sulfide ameliorated high choline-induced cardiac dysfunction by inhibiting cGAS-STING-NLRP3 inflammasome pathway. Oxid Med Cell Longev 2022: 1392896, 2022.
76. Gong W, Zhang S, Chen Y, Shen J, Zheng Y, Liu X, Zhu M and Meng G: Protective role of hydrogen sulfide against diabetic cardiomyopathy via alleviating necroptosis. Free Radic Biol Med 181: 29-42, 2022.
77. Qin M, Long F, Wu W, Yang D, Huang M, Xiao C, Chen X, Liu X and Zhu YZ: Hydrogen sulfide protects against DSS-induced colitis by inhibiting NLRP3 inflammasome. Free Radic Biol Med 137: 99-109, 2019.
78. Gao Y, Zhang H, Wang Y, Han T, Jin J, Li J, Tang Y and Liu C: L-cysteine alleviates myenteric neuron injury induced by intestinal ischemia/reperfusion via inhibitin the macrophage NLRP3-IL-1β pathway. Front Pharmacol 13: 899169, 2022.
79. Zhang N, Zhou Z, Huang Y, Wang G, Tang Z, Lu J, Wang C and Ni X: Reduced hydrogen sulfide production contributes to adrenal insufficiency induced by hypoxia via modulation of NLRP3 inflammasome activation. Redox Rep 28: 2163354, 2023.
80. Fan J, Zheng F, Li S, Cui C, Jiang S, Zhang J, Cai J, Cui Q, Yang J, Tang X, *et al*: Hydrogen sulfide lowers hyperhomocysteinemia dependent on cystathionine γ lyase S-sulfhydration in ApoE-knockout atherosclerotic mice. Br J Pharmacol 176: 3180-3192, 2019.
81. Yang K, Coburger I, Langner JM, Peter N, Hoshi T, Schönherr R and Heinemann SH: Modulation of K^+ channel N-type inactivation by sulfhydration through hydrogen sulfide and polysulfides. Pflugers Arch 471: 557-571, 2019.
82. Luo S, Kong C, Ye D, Liu X, Wang Y, Meng G, Han Y, Xie L and Ji Y: Protein persulfidation: Recent progress and future directions. Antioxid Redox Signal 39: 829-852, 2023.
83. Wu Q, Zhao B, Weng Y, Shan Y, Li X, Hu Y, Liang Z, Yuan H, Zhang L and Zhang Y: Site site-specific quantification of persulfidome by combining an isotope-coded affinity tag with strong cation-exchange-based fractionation. Anal Chem 91: 14860-14864, 2019.
84. Bibli SI, Hu J, Sigala F, Wittig I, Heidler J, Zukunft S, Tsilimigras DI, Randriamboavonjy V, Wittig J, Kojonazarov B, *et al*: Cystathionine γ lyase sulfhydrates the RNA binding protein human antigen r to preserve endothelial cell function and delay atherogenesis. Circulation 139: 101-114, 2019.
85. Luo S, Kong C, Zhao S, Tang X, Wang Y, Zhou X, Li R, Liu X, Tang X, Sun S, *et al*: Endothelial HDAC1-ZEB2-NuRD complex drives aortic aneurysm and dissection through regulation of protein S-sulfhydration. Circulation 147: 1382-1403, 2023.
86. Wu D, Tan B, Sun Y and Hu Q: Cystathionine γ lyase S-sulfhydrates Drp1 to ameliorate heart dysfunction. Redox Biol 58: 102519, 2022.
87. Altaany Z, Ju Y, Yang G and Wang R: The coordination of S-sulfhydration, S-nitrosylation, and phosphorylation of endothelial nitric oxide synthase by hydrogen sulfide. Sci Signal 7: ra87, 2014.